Initialization of the JYFLTRAP system

Toni Tapani Pikkarainen

UNIVERSITY OF JYVÄSKYLÄ

Master´s thesis
University of Jyväskylä, Physics department
February 28, 2013
Supervisors: Dr. Veli Kolhinen
Prof. Dr. Ari Jokinen

Contents

Abstract

The IGISOL facility has been moved into a new location at the acceleration laboratory of the University of Jyväskylä. The superconducting magnet that is part of the JYFLTRAP system has been re-energized. In this thesis a commissioning of the Penning trap apparatus JYFLTRAP is described. This involves a precise alignment of the structure of the trap along field lines of strong solenoid field. The alignment was completed successfully with a special alignment device. In addition, some improvements were done for the Penning traps and transfer line from RFQ cooler, and a buncher to the injection of Penning traps was built during this project.

Tiivistelmä

Jyväskylän yliopiston IGISOL-ryhmän laboratorio on muutettu fysiikan laitoksen kiihdytinlaboratorion sisällä uusiin tiloihin. IGISOL-laitteistoon kuuluu 7 Teslan suprajohtava solenoidi, joka laboratorion muuton yhteydessä on ensin kytketty pois päältä ja sitten käynnistetty uudelleen. Suprajohtava solenoidi ja sen sisällä olevat kaksi Penningin loukkua ovat osa JYFLTRAPiksi nimettyä loukkujärjestelmää. Tässä tutkielmassa esitellään toimenpiteet, jotka tehtiin Penningin loukku -laitteiston käyttöönottoa varten.
Solenoidin käynnistämisen jälkeen sen sisällä oleva tyhjiöputki linjattiin tarkasti samansuuntaiseksi magneettikentän kenttäviivojen kanssa. Linjaukseen käytettiin erityisesti tähän tarkoitukseen suunniteltua linjauslaitetta.
Penningin loukkuihin tehtiin muutamia parannuksia, ennen kuin ne laitettiin tyhjiöputkeen solenoidin sisälle. Lisäksi suihkulinja radiotaajuuskvadrupolilta Penningin loukkujen injektiopuolelle rakennettiin tämän projektin aikana.

1 Introduction

In the experimental nuclear physics properties of atomic nuclei are being researched. Nowadays properties of stable isotopes are well-known and therefore the experiments are focused on exotic nuclei. These kind of nuclei can be produced by colliding an ion beam, produced with particle accelerator, to a target. An exotic nucleus is a nucleus with a large amount of protons or neutrons and this kind of nuclei are usually very unstable. Thus, one problem in studying exotic nuclei is to extract them out of the target as fast as possible.

At Cern, an ISOL (Isotope Separator On-Line) method [1] has been used to produce radioactive ion beams. The primary beam is directed into a thick target and the reaction products are stopped in the bulk of the target material. After that the produced nuclides are diffused out of the target and ionized. With this method the release time of the produced nuclides depends on the chemical properties of the nuclides.

At the University of Jyväskylä an IGISOL (Ion Guide Isotope Separator On-Line) -technique has been used to study exotic nuclei since 1980s [2]. The radionuclides are produced by bombarding a thin target with the primary beam. The recoil nuclides are stopped in a buffer gas and extracted out with help of gas jet and electric fields. With the IGISOL technique the release time does not depend on the chemical properties of the nuclides and it is possible to extract all nuclides quite fast.

A trap system called JYFLTRAP has been attached to the IGISOL -facility and this system allows an ion separation on an isobaric level. An isobar means a group of nuclei with the same mass number but a different amount of protons and neutrons. The JYFLTRAP consists of two Penning traps which are located inside the same magnet. The first trap is used for the isobaric purification of an ion beam and the second trap is for the precision mass measurements.

For a proper operation of the Penning traps the quality of the beam has to be improved. A radio frequency quadrupole (RFQ) cooler and buncher has been developed for this purpose. In addition, it is possible to bunch the ion beam with the RFQ.

Inside the bore tube of the magnet the Penning traps are located in a vacuum tube. For a proper operation of the Penning traps the trap structures must be aligned along the magnetic field lines. If the electric field is not coaxial with

the magnetic field there will be systematic errors in the mass measurements of nuclei.

2 Beam quality and ion optics

2.1 Energy spread

When an ion beam is accelerated with an electric field it is easy to calculate an average energy for the beam if the charge of the ions is known. In reality some of the ions have lower or higher energy compared to the average energy. This phenomenon is called energy spread of the ion beam. The energy spread may cause errors to the time-of-flight measurements and thus it should be minimized. At the IGISOL facility the energy spread of an ion beam is lowered by bunching and cooling the beam with the RFQ cooler. Typical unit for the energy spread is electron volt (eV).

2.2 Emittance

In addition to the longitudinal energy spread an ion beam has always transversal momentum and position spreads. A quantity called emittance is used to describe the beam quality. A smaller emittance means a better beam quality. Emittance is defined as $\epsilon = \Delta x \Delta p_x / p_0$ [3] where $\Delta x \Delta p_x$ is the phase space area the of beam (in x-direction) and p_0 is the momentum of a reference ion travelling along the optical axis. Usually the value of emittance is given in mm mrad units. According to Liouville´s theorem [4] the phase space area remains constant in conservative force fields. In addition to the value of emittance one can show the action diagram of the beam. With action diagrams it is easier to understand whether the beam is diverging or converging. An action diagram is shown in Figure 1.

Normally the z-direction is defined as the optical axis of the beam. In the first graph of Figure 1 majority of the particles having negative x-coordinate have positive momentum in x-direction and vice versa so the beam is converging. In the second graph the beam is parallel and in the third graph it is diverging. In the reality an action diagram resembles an ellipse instead of a square.

2.3 Cooling

When an ion beam is cooled it means that its phase space area is decreased. Due to the fact that in conservative force fields the phase space area $\Delta x \Delta y \Delta z$ $\Delta p_x \Delta p_y \Delta p_z$ remains constant non-conservative force fields are needed for cooling. A buffer gas cooling is used at the IGISOL facility. In this method the ions are colliding with buffer gas atoms. Due to the friction force between ions and atoms the phase space area of the beam particles is decreased. [3]

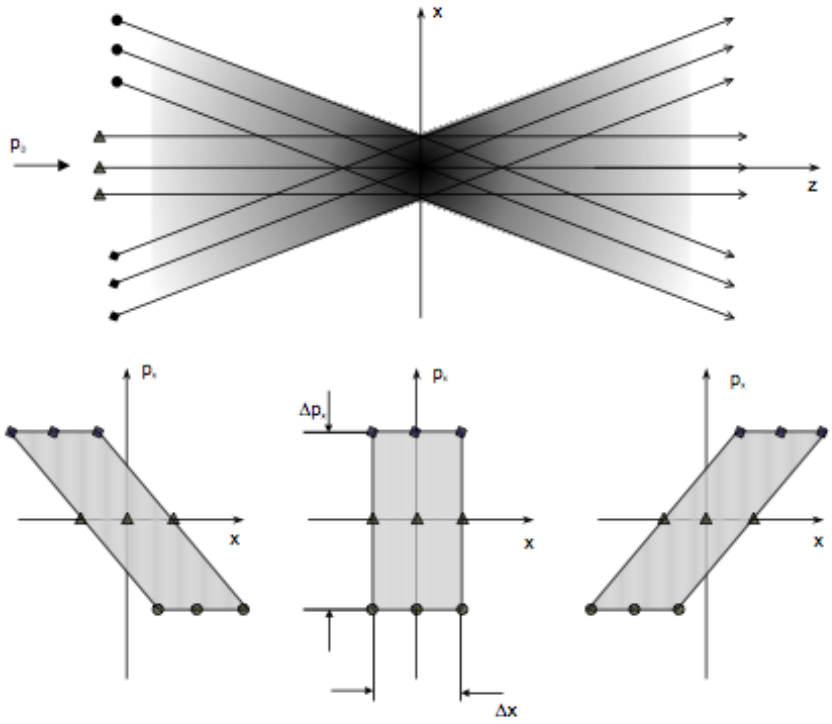

Figure 1: An action diagram of an ion beam.

2.4 Ion optics

2.4.1 An Einzel lens

An Einzel lens is an ion optical element and it is used to focus ion beams. It consists of three cylindrical electrodes of which two outermost are in the same potential. Also double cylinder electrostatic lenses have been used. [5] In addition to handling low energy ion beams Einzel lenses are used in electron microscopes.

In the beam line of the IGISOL, Einzel lenses are used to focus positively charged beam particles. The outermost electrodes are connected to ground and the middle electrode is connected to desired voltage as it is shown in Figure 2.

The voltage in the middle electrode of an einzel lens is typically less than half of the beams energy. The higher the voltage is the stronger is the focusing effect. For example in the IGISOL beamline from RFQ to Penning traps the beam has energy of 800 eV and the simulated values for the voltages of the Einzels vary from 210 V to 330 V.

With Einzel lenses it is only possible to focus the ion beams. If the beam is misaligned from the optical axis the direction of propagation needs to be changed. For that purpose other elements are used.

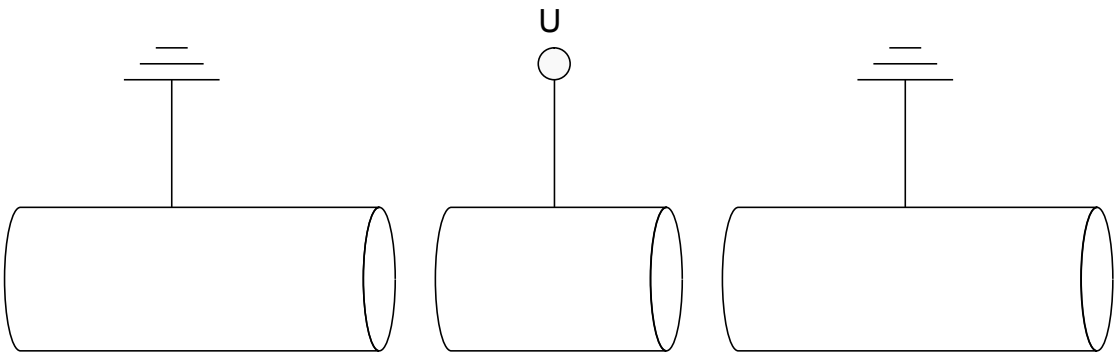

Figure 2: An Einzel lens. Two outermost electrodes are connected to ground and the middle electrode is connected to either positive or negative voltage.

2.4.2 XY-steerer

An xy-steerer is an ion optical element consisting of four plate electrodes, as shown in Figure 3. There are two plates in both x- and y-directions and voltages are applied between them. With x-steerers it is possible to bend the beam horizontally and with y-steerers vertically. By changing the polarity of the voltage it is possible to change the direction of the steering.

At the IGISOL facility a power supply with maximum output of the order of 1 kV is typically used for xy-steerers. With a double xy-steerer it is possible make a parallel shift for an ion beam. In the beam line from the RFQ to the Penning traps there are three double xy-steerers. These have to be used if the propagation direction of the beam is misaligned from the optical axis.

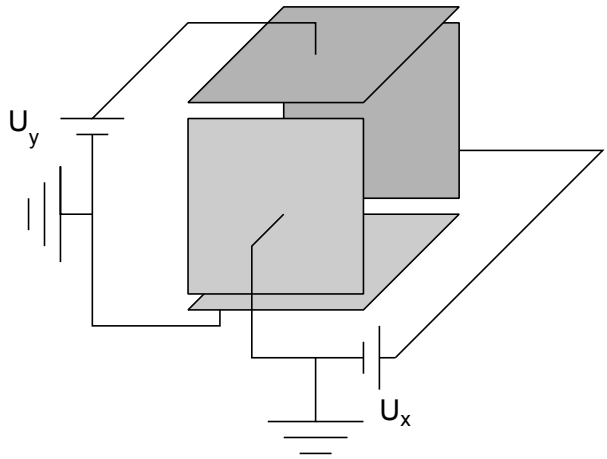

Figure 3: An xy-steerer.

3 IGISOL technique

IGISOL (Ion Guide Isotope Separator On-Line) technique is based on gas stopping of reaction recoils and extraction of the recoils by gas flow. This technique allows fast extraction of the produced radionuclides. In addition to decay spectroscopy, the properties of these nuclei can be studied by collinear laser spectroscopy and ion trap techniques. [2]

In the IGISOL method the secondary radioactive beam is produced by di-

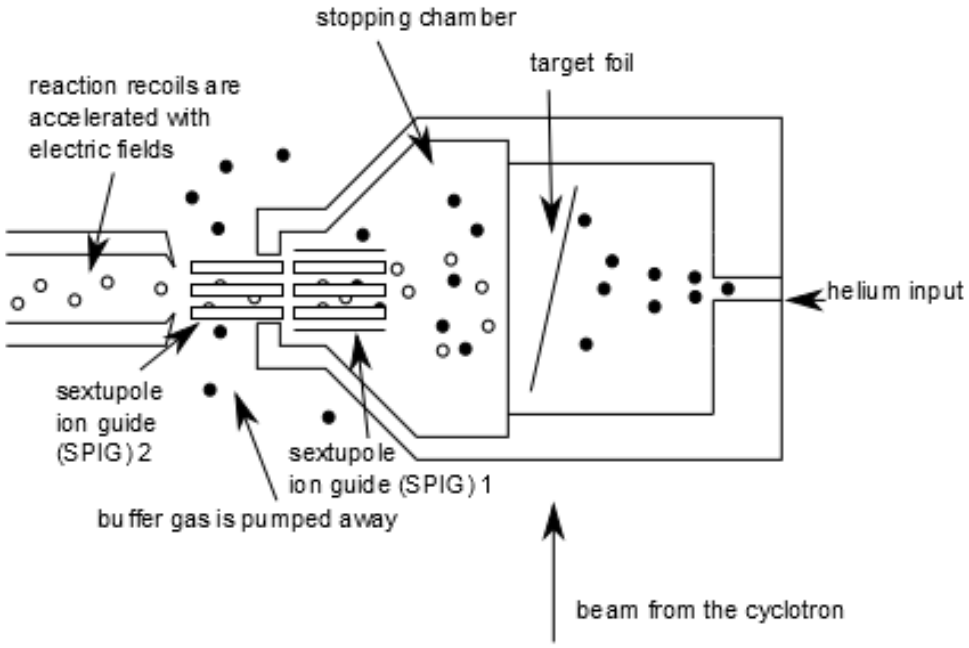

Figure 4: The target chamber of the IGISOL facility.

recting a primary beam from the cyclotron to a target. Typically the primary beam consists of protons and the target is a thin uranium foil. The target chamber is shown in Figure 4.

In the target chamber the reaction recoils are slowed down and thermalized in gas which is usually helium [6], but sometimes argon [2]. Charge states of the produced nuclides are initially quite high but they are fast reseted to lower charge states via charge-exchange processes with buffer gas atoms. If

the buffer gas is pure helium many radioactive ions can remain in the 2^+ charge state. For many isotopes the second ionization potential is below the first ionization potential of helium [2]. However, in a real buffer gas there is small amount of impurities of other gas atoms which cause the majority of the radioactive ions to reach the 1^+ charge state.

After the thermalization and the charge exchange processes to 1^+ states the ions are extracted out of the gas cell by gas flow. For the transportation of the extracted ions a sextupole ion guide (SPIG) [7] is used. The beam is guided through a differentially pumped electrode system and accelerated up to the energy of 40 keV. The beam line after the gas cell has to be in high vacuum. The buffer gas is pumped away from the target chamber with effective Roots blower pumps. The subsequent pumping section ensures the 10^{-6} mbar pressure in the beam lines.

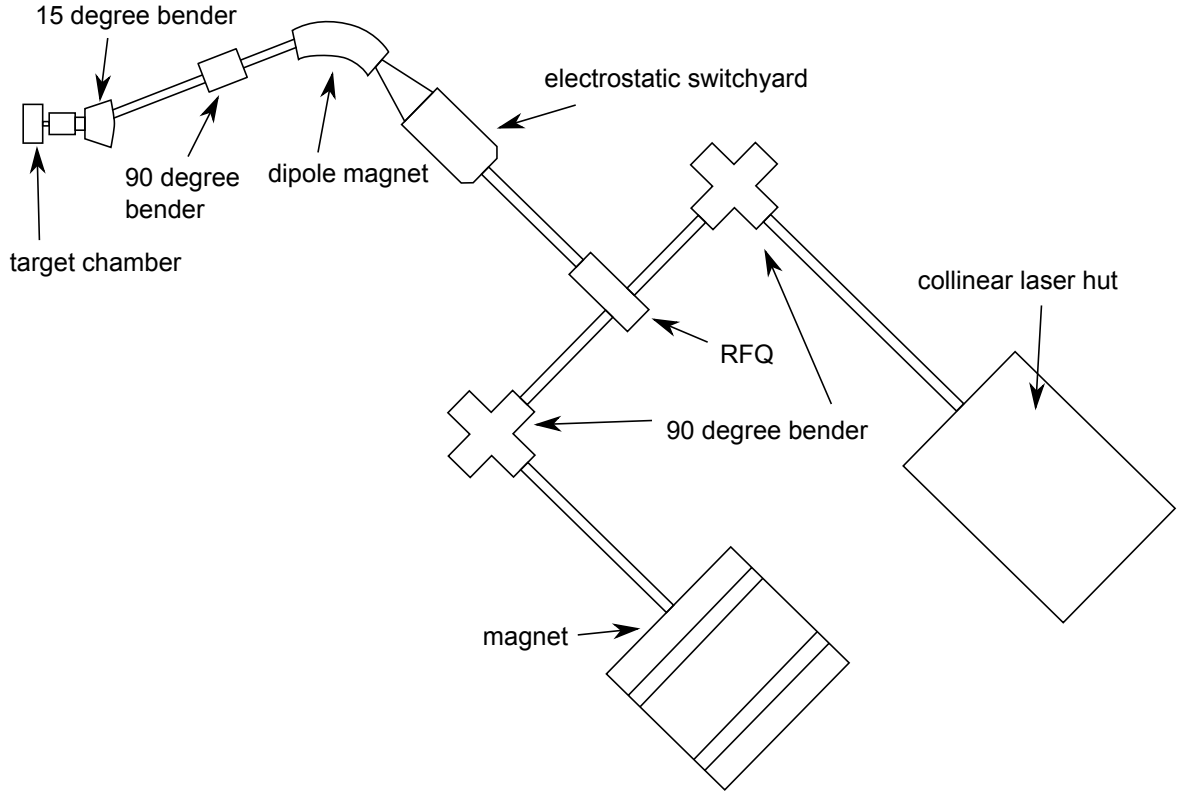

Figure 5: The schematic layout of the IGISOL laboratory.

After the beam is extracted from the ion guide the beam particles are guided through an analyzing dipole magnet as it is shown in Figure 5. The dipole magnet is used for a rough mass separation of the beam paricles. A magnet causes a force for a moving charged particle. It is derived as [8]

$$\vec{F} = q\vec{v} \times \vec{B}, \tag{1}$$

where $\vec{F}$ is the force, $\vec{B}$ the magnetic field density, q the charge and $\vec{v}$ the velocity of the particle. The magnet is installed so that the propagation direction of the beam is perpendicular to the magnetic field lines. Due to the cross product in equation (1) the direction of force on the particles is perpendicular to both the velocity and the magnetic field density vectors. Now it is possible to write the equation (1) in scalar form

$$ma = qvB, \tag{2}$$

and again

$$m\frac{v}{r} = qB, \tag{3}$$

using the formula $a = \frac{v^2}{r}$ for central acceleration a. As a significant fraction of the ions has been reseted to the 1^+ charge state the bending radius r of an ion is mostly dependent on its mass m and the magnetic field density B. A schematic drawing of the mass separation with the dipole magnet is shown in Figure 6. At the end of the magnet there is a narrow slit and by changing the magnetic field density it is possible to choose which ions will pass through the slit. Typical mass resolving power of the dipole magnet $R = \frac{m}{\Delta m}$ is of the order of 250-500 [6] allowing separation of ions by mass number.

4 Radio Frequency Quadrupole (RFQ) cooler

After the beam has been extracted out of the target chamber and directed through the dipole magnet it still has quite large energy spread and emittance. The energy spread is of the order of 50-150 eV and the emittance is of the order of $10\pi - 15\pi$ mm mrad [3]. For reducing these values and improving the quality of the beam a RFQ cooler is positioned next in the beam line. For the injection into the Penning traps the beam is needed to be converted to ion bunches and this can be done with the RFQ cooler. [9]

The RFQ is a linear Paul trap [10]. This type of trap captures the ions only with electric fields. The RFQ cooler is placed on a high voltage platform because the ions have to be slowed down for the injection to the cooler. As the

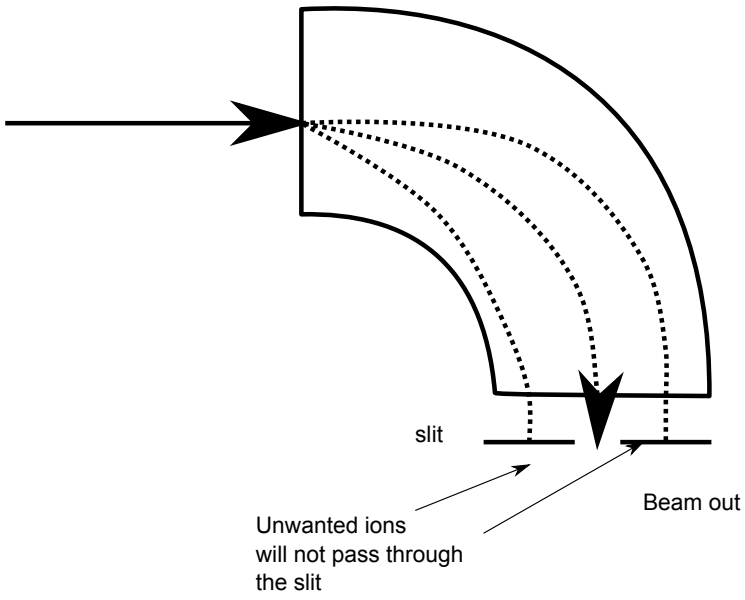

Figure 6: A schematic drawing of a dipole magnet.

beam is slowed down it also has to be focused into the quadrupole. It is done with two cylindrical electrostatic lenses and without these elements the beam would be diverging strongly.

The quadrupole is placed in a buffer gas cell and it consists of four 40 cm long, parallel, cylindrical rods which are divided in 16 segments. Ions are trapped in radial direction by applying an oscillating RF voltage on the rods. In axial direction the ions are trapped in electric potential well. Ions are transported through the cooler by creating a weak electric field towards the extraction end of the device. That field is created by applying DC voltages to segments of the rods. As a positive voltage is applied to the end plate, the bottom of the potential well is at the extraction end of the cooler as it is shown in Figure 7.

The axial and the radial energy of the injected ions is reduced in collisions with the buffer gas atoms. The ions are kept in the optical axis with the radiofrequency electric field and drawn at the extraction end where they are accumulated typically few hundred milliseconds. An ion bunch with width of 10-20 μs is released by lowering the voltage in the end plate for 100 μs.

After the ions are manipulated in the RFQ device the quality of the beam is highly improved and the beam is directed forward as bunches. The energy spread after the cooler is 1 eV and the emittance is 3π mm mrad [3], [9].

5 Principle of a Penning trap

A Penning trap is a trap for ions and the trapping is achieved by a combination of magnetic and electrostatic fields [10]. Penning traps were already used in 1940s to trap ions and to measure their charge-to-mass ratios [11]. Currently, Penning traps can be used for an isobaric separation of ions and for accurate mass measurements.

In an ideal Penning trap there is a homogenous magnetic field coaxial to an electrostatic quadrupole field. The superposition of these fields allows an ion to be stored inside the trap. An electrostatic quadrupole field can be obtained by using two endcaps and a ring electrode which all are hyperbolical as shown in Figure 8. The endcaps are in the same potential and there is a potential difference U_0 between them and the ring electrode. With hyperbolical configuration the shape of the quadrupole field is determined by the electrode geometry. Another option for creating such a field is to use cylindrical electrodes that have a certain length to radius ratio and apply certain

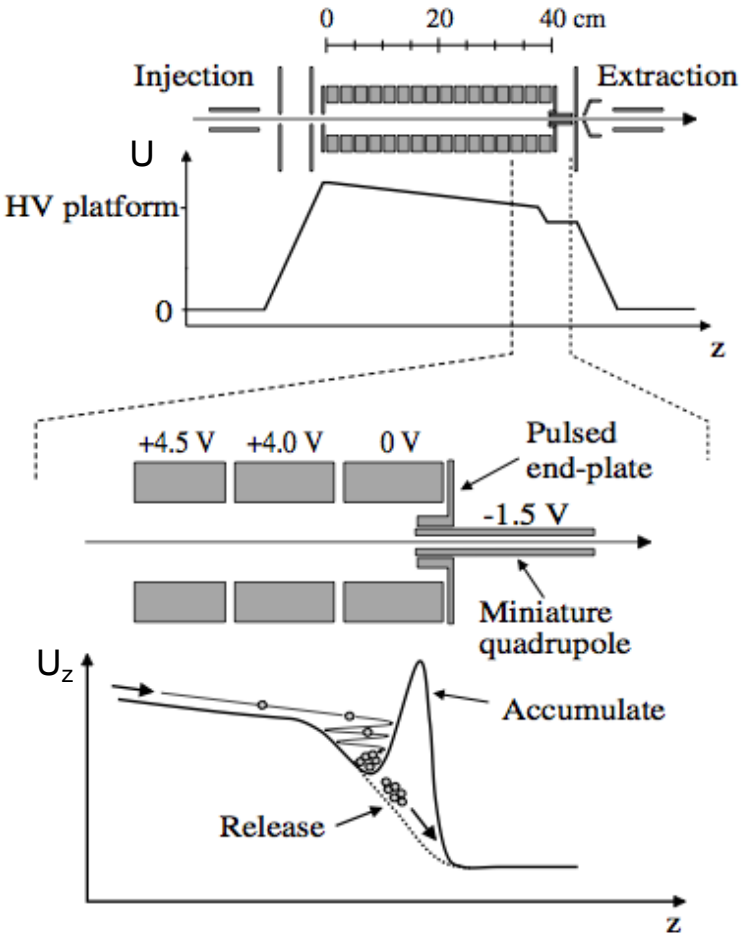

Figure 7: A working principle of the RFQ cooler. The ions are confined in radial direction with the RF electric field and cooled in collisions with the buffer gas atoms. In axial direction a potential well is created at extraction end of the cooler and ions are released from the well by lowering the voltage of the end plate. [9]

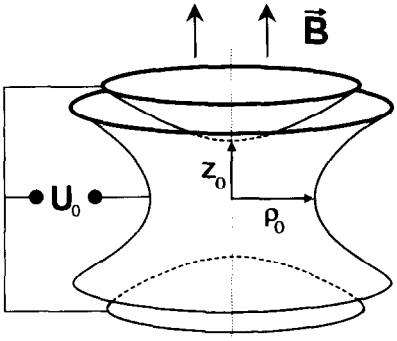

Figure 8: An illustration of an ideal hyperbolical Penning trap.

voltages on them. Structure of a cylindrical trap is illustrated in Figure 9. Correction electrodes are needed in both configurations to compensate the field imperfections.

5.1 Ion motion inside a Penning trap

A motion of a charged particle inside a Penning trap consists of three different eigenmotions. A potential U_0 creates an axial oscillation with a frequency [12]

$$\omega_z = \sqrt{\frac{qU_0}{md^2}} \tag{4}$$

where q and m are the charge and mass of the trapped ion and d is so called characteristic trap parameter. d depends on the trap geometry and is determined by

$$4d^2 = (2z_0^2 + \rho_0^2) \tag{5}$$

where z_0 is the distance from the trap center to endcap electrodes and ρ_0 is the radius of the ring electrode.

If there were no electric field the motion of a stored ion in the magnetic field B would be pure cyclotron motion with a frequency

$$\omega_c = \frac{q}{m}B\,. \tag{6}$$

However the quadrupole electric field causes the ion motion to become a superposition of three different eigenmotions as illustrated in Figure 10. The motion with lower frequency ω_- is called magnetron motion. The other radial motion having higher frequency ω_+ is called reduced cyclotron motion.

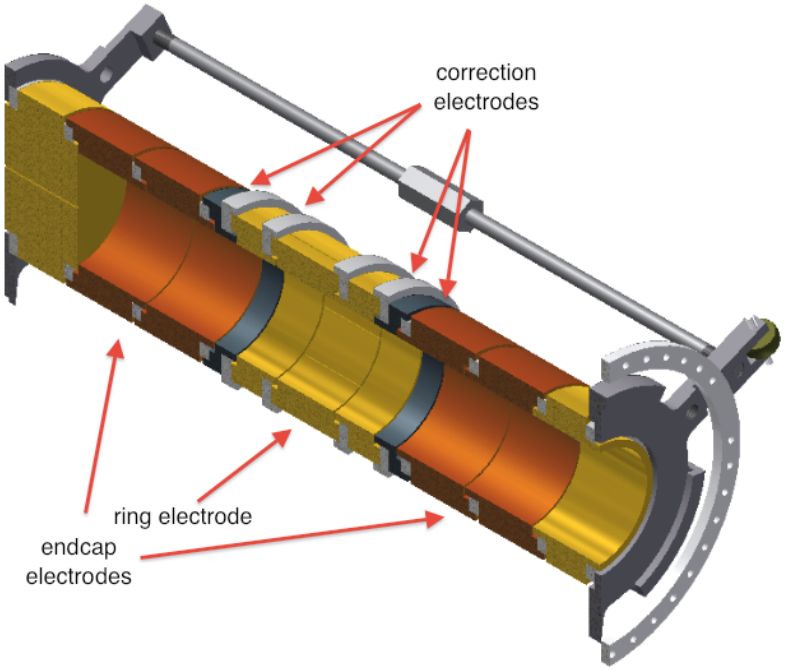

Figure 9: A cylindrical Penning trap.

The magnetron frequency and the reduced cyclotron frequency are derived as

$$\omega_{\pm} = \frac{\omega_c}{2} \pm \sqrt{\frac{\omega_c^2}{4} - \frac{\omega_z^2}{2}}\,. \tag{7}$$

In an ideal trap the sum of these frequencies

$$\omega_- + \omega_+ = \omega_c \tag{8}$$

is equal to the real cyclotron frequency.

5.2 Imperfections in a real Penning trap

In a real Penning trap geometrical imperfections of the trap are a source of many systematic errors. For example the holes in the endcap electrodes might cause deviations from the pure quadrupole electric field. Usually correction electrodes are used to minimize these errors.

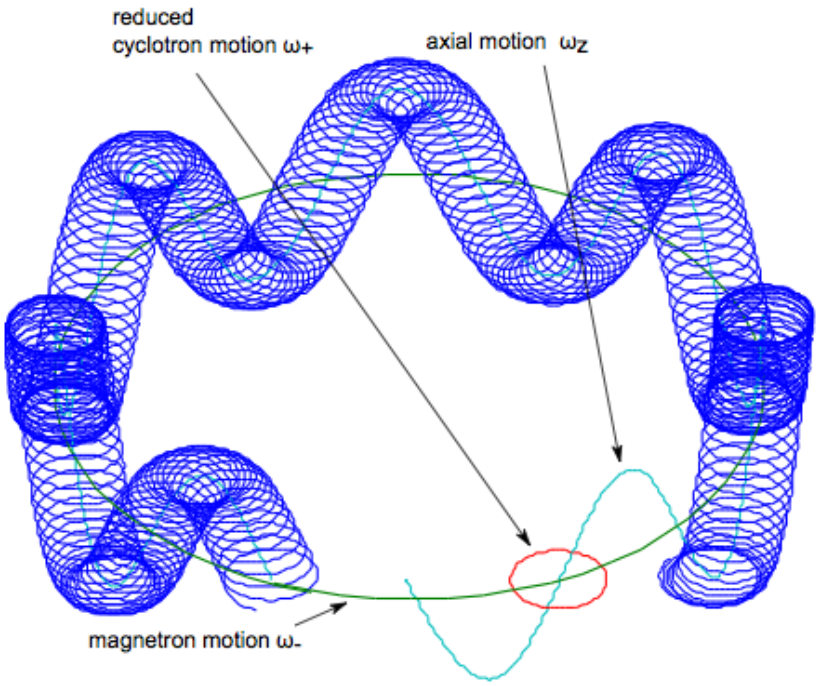

Figure 10: Ion motion in a Penning trap is illustrated. Motion consists of the three eigenmotions of the ion. Frequencies $\omega_- = 1{,}735$ kHz, $\omega_+ = 600$ kHz and $\omega_z = 13$ kHz were used to create this plot.

Another source of systematic errors is the misalignment of the Penning trap. The aim of the alignment was to minimize the tilting between the trap axis and the magnetic field axis. If the trap is misaligned there will be shifts in the eigenfrequencies. It is found that these frequency shifts are mass independent and they can cause systematic errors to the mass measurements. [12]

The size of the frequency shifts caused by the trap imperfections depends on the amplitudes of ion motions. Several cooling methods have been developed to minimize the errors. [13]

6 JYFLTRAP

The JYFLTRAP consists of the RFQ cooler and two Penning traps which are situated inside the same 7-T superconducting solenoid. The technical drawing of the new beam line from the RFQ to the magnet is shown in Figure 11. The

Penning traps inside the magnet are shown in Figure 12. Both traps consist of cylindrical electrodes. The first trap is used for isobaric purification and the second one is for precision mass measurements. The trap electrodes are illustrated in Figure 13.

After the magnet was mounted in the new location it was energized and shimmed. Shimming means finetuning of the magnetic field by placing ferromagnetic metal strips around the bore tube. The goal of the shimming process was to create two homogeneous 1 cm^3 regions 10 cm apart from the center of the magnet. The homogeneity of the magnetic field, $\frac{\Delta B}{B}$, is 1,57 ppm (parts per million) in the region of the purification trap and 0,28 ppm in the precision trap region.

After the shimming of the magnet the beamline, shown in Figure 11, was built. The ion optics were inserted inside the chambers and aligned. The goal of the alignment was to adjust the center of the ion optical elements on the same optical axis. Vertical coordinate of the optical axis was obtained by a line drawn on the wall. There was also a line drawn on the floor which allowed the obtaining of the horizontal coordinate. The alignment was done with a special camera.

6.1 Injection of the ions to the Penning traps

From the RFQ the ions are directed to the Penning traps. The quality of the beam is ideal for the injection in to the traps because ions are moving as bunches and energy spread is less than 1 eV. The cooler and the Penning traps are located on the same high voltage platform. The beamline between the cooler and the traps is also on the same high voltage platform but the voltage of the line is lowered 900 V for the transportation of the ions. [14]

When the trap is closed the depth of the potential well in the purification trap is 100 V [15]. For the injection of an ion bunch into the trap the voltages of the injection side trap electrodes are lowered. After the ion bunch is inside the trap the injection side potential wall is closed again. The energy of the bunch is adjusted to be few electron volts higher than the energy of the ring electrode, which is the segmented electrode in the middle of the purification trap. There is also a ring electrode in the precision trap and the structure of a ring electrode is shown in Figure 14.

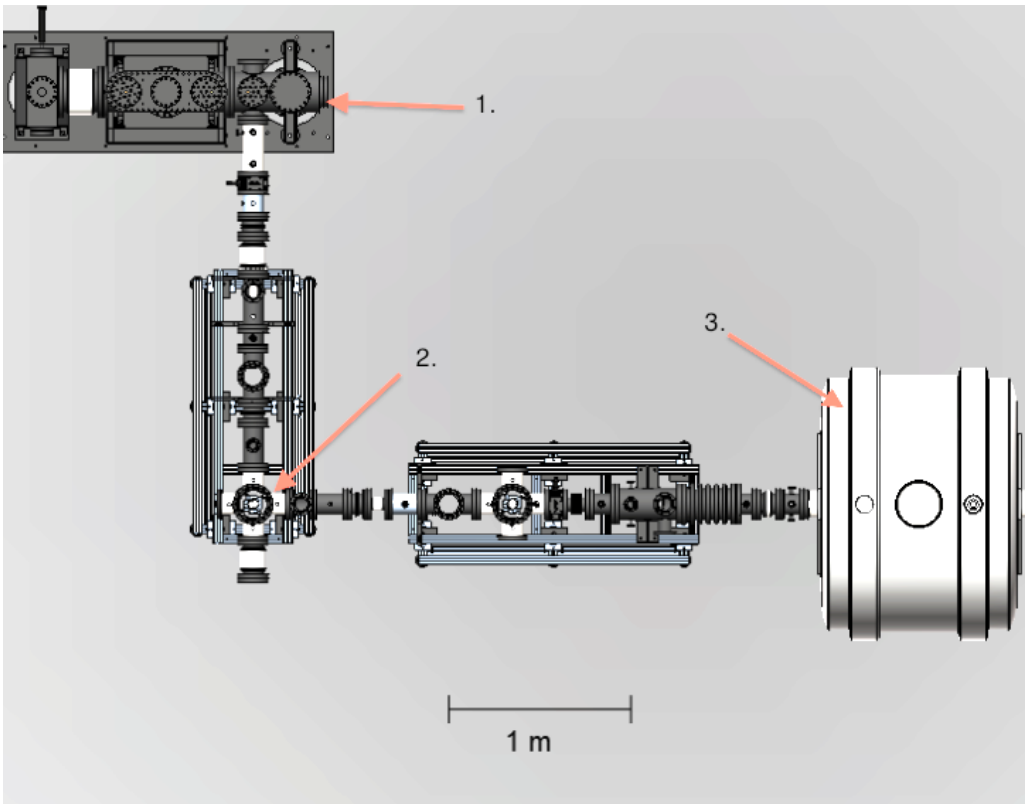

Figure 11: The beam line from the RFQ to the magnet. 1. RFQ 2. 90 degree quadrupole bender. 3. Superconducting solenoid. There are several ion optical elements in that line which are listed in Figure 41.

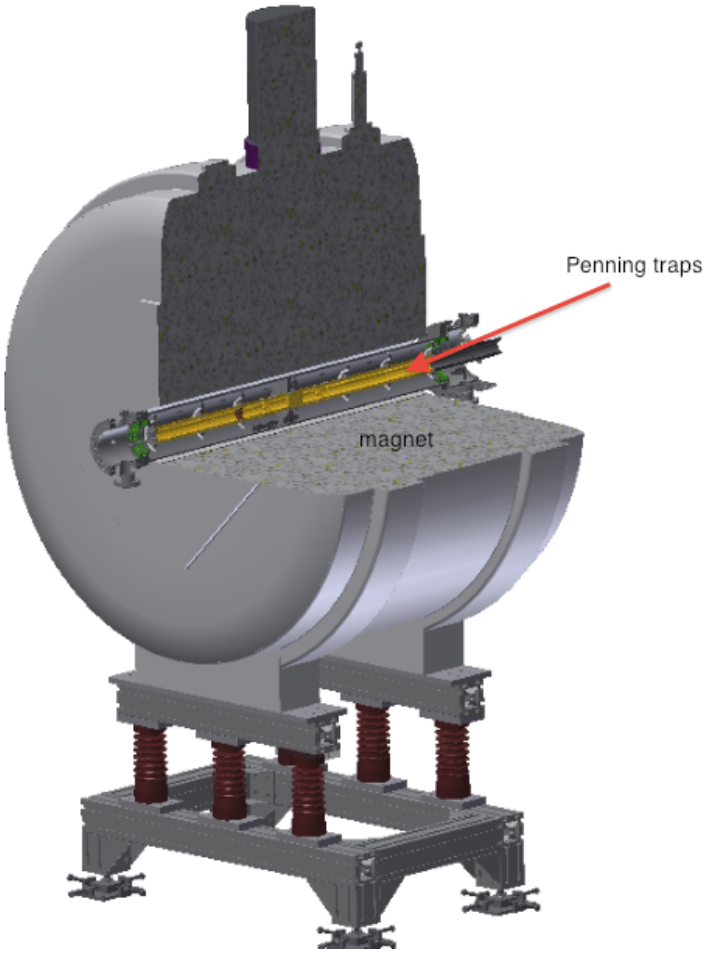

Figure 12: The Penning traps inside the magnet are illustrated.

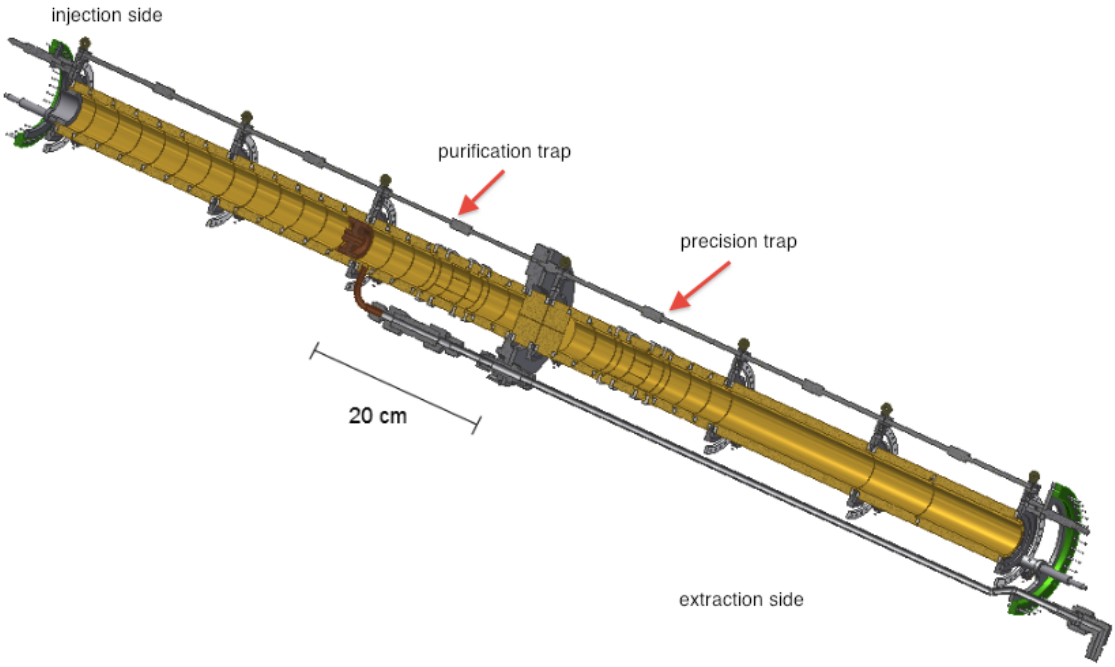

Figure 13: All trap electrodes are illustrated.

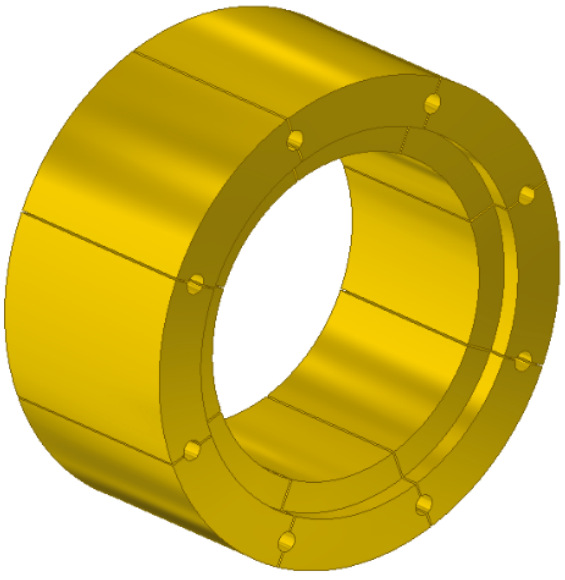

Figure 14: Ring electrodes in the both traps of the JYFLTRAP system consist of eight electrode segments.

6.2 Purification trap

A drawing of the purification and the precision trap is shown in Figure 15. Inside the purification trap there is buffer gas which causes the cooling of the injected ions. The buffer gas flow out of the purification trap is minimized with use of electrodes having small diaphraghms. Between the traps there is a pumping barrier which is needed to achieve high enough vacuum in the precision trap. The buffer gas is fed into the purification trap through the gasline which is also illustrated in Figure 15. The accurate electrode structure of the purification trap is shown in Figure 16.

Ions are cooled until the axial motion is limited inside the ring electrode. When buffer gas pressure is of the order of 10^{-4} mbar the axial cooling takes few hundred milliseconds. Also the radial eigenmotions of the ions are cooled but the reduced cyclotron motion with higher frequency is cooled faster than the magnetron motion. In the cooling process the radius of the reduced cyclotron motion decreases and the radius of the magnetron motion increases as it is shown in Figure 19.

6.2.1 Dipole excitation

Buffer gas -cooling technique is used to damp the axial and the reduced cyclotron motions away. After these eigenmotions have been cooled away, it is possible to start the excitations of the ions with the radiofrequency electric fields. The goal is to accomplish isobaric mass separation for the ions. The RF electric fields are created by applying oscillating RF voltages to the segments of the ring electrode.

First step in manipulation of the ion motions is the dipole excitation. The dipole excitation is accomplished by applying oscillating voltages to the opposite halves of the ring electrode. In dipole excitation the opposite halves have the same frequency and amplitude but opposite phase. In JYFLTRAP the dipole excitation is simplified in a way that the voltage is applied to only one quadrant (two neighboring octants) at a time while others are grounded. This method works properly because the voltage in the one quadrant is by turns higher and lower compared to the grounded ones. The connections for dipole and quadrupole excitations are illustrated in Figure 17.

With the dipolar oscillating electric field it is possible to excite either the reduced cyclotron motion or the magnetron motion depending on the oscillation frequency. The magnetron motion is excited using magnetron frequency f_- as the oscillation frequency so the radius of the magnetron motion is in-

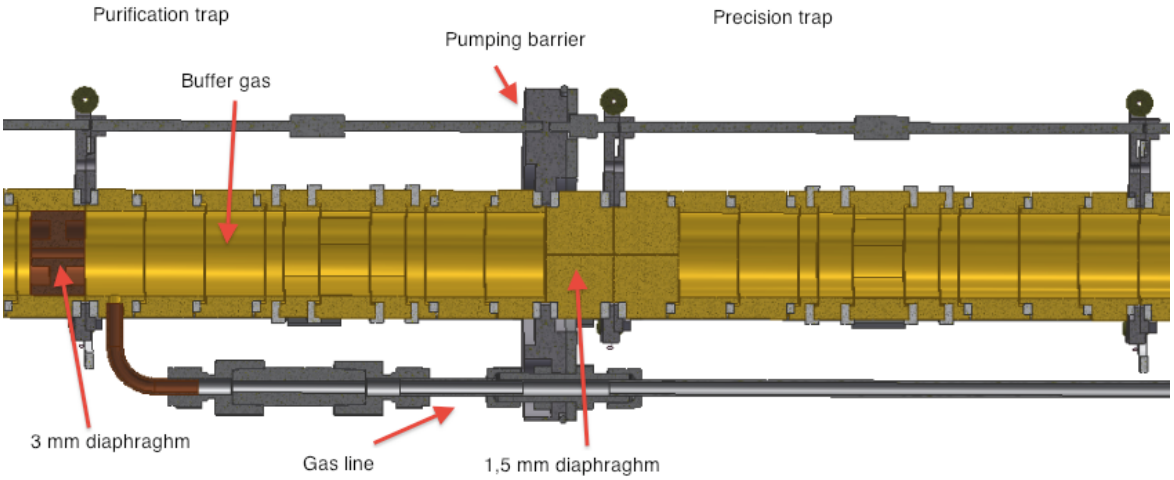

Figure 15: Both Penning traps of JYFLTRAP are illustrated.

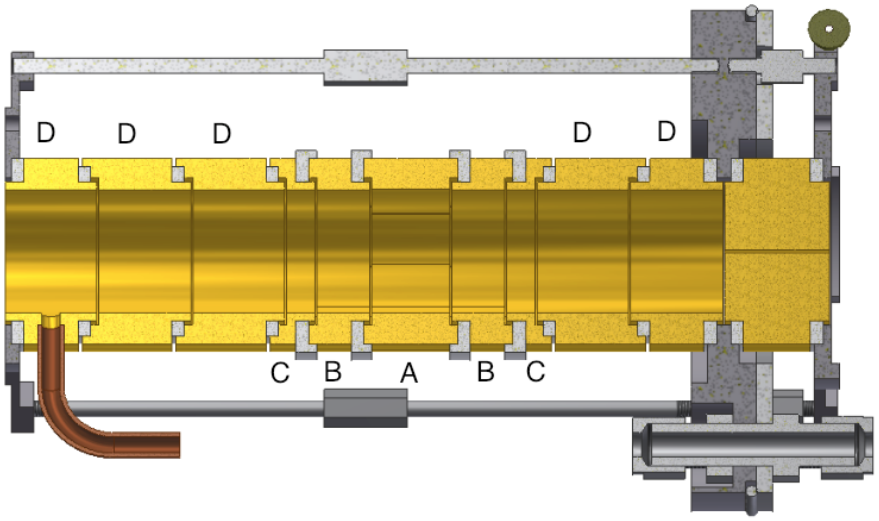

Figure 16: The electrode structure of the purification trap. The electrode structure of the precision trap is a mirror image of the purification trap as it is seen in Figure 15. In both traps there are a ring electrode (A), inner correction electrodes (B), outer correction electrodes (C) and endcap electrodes (D).

creased. It has been observed that the magnetron frequency is almost mass independent so with magnetron excitation all ions can be removed from the trap center. If the excitation is done with the eigenfrequency of the reduced cyclotron motion f_+ which is mass dependent, only ions that have this particular reduced cyclotron frequency are removed from the trap center.

The eigenfrequency of the magnetron motion at the purification trap of JYFLTRAP is approximately 1700 Hz [10]. It has been obtained by scanning the extracted ions as a function of the excitation frequency. When the excitation frequency is equivalent to the eigenfrequency there are no ions coming out from the traps due to the fact that they will not pass through the small diaphraghm at the endcap electrode of the purification trap.

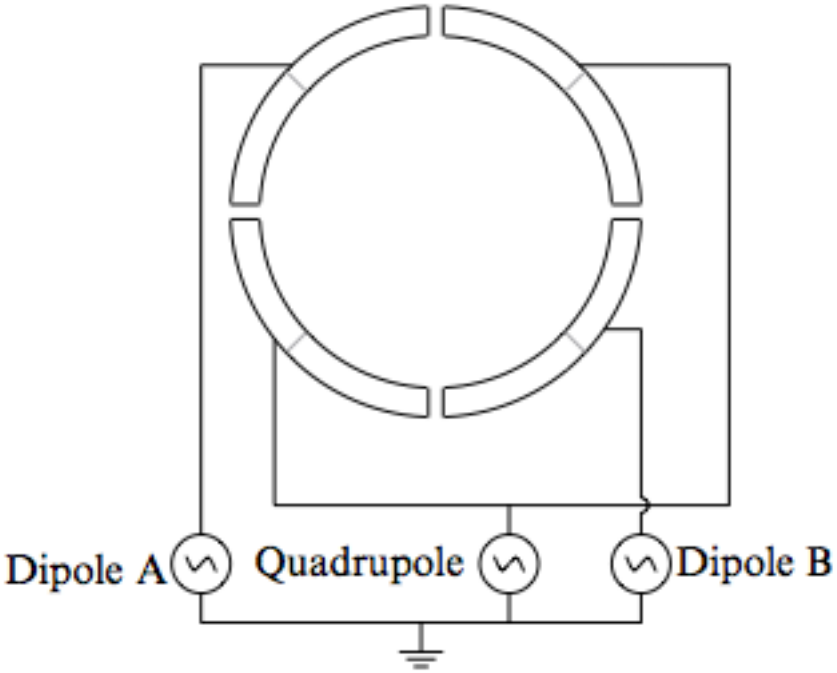

Figure 17: A schematic drawing of the ring electrode at the both purification and the precision traps. The ring electrode consists of eight segments and octants are transferred in to quadrants by connecting two neighboring octants together. At JYFLTRAP, two of quadrants are used for quadrupole excitation and Dipole A is for magnetron and Dipole B for reduced cyclotron motion excitation. [14]

6.2.2 Quadrupole excitation

Quadrupole excitation is accomplished by applying oscillating voltage with same frequency, amplitude and phase in two opposite quadrants and connecting other two quadrants to the ground as it is shown in Figure 17. If the frequency of the voltage is the cyclotron frequency $\omega_c = \omega_- + \omega_+$ the excitation will convert the magnetron motion into reduced cyclotron motion or other way around. The conversion is illustrated in Figure 18.

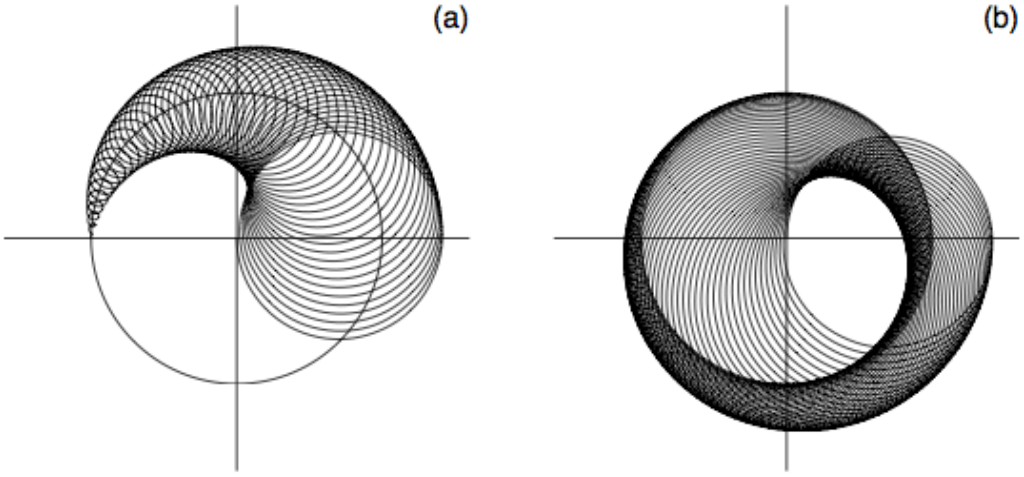

Figure 18: If the quadrupole excitation frequency is equivalent to the cyclotron frequency ω_c, (a) magnetron motion is converted into reduced cyclotron motion or, (b) reduced cyclotron motion is converted into magnetron motion. [3]

6.2.3 Purification cycle

At the purification trap of JYFLTRAP, one isobar is wanted to separate from others. With help of the buffer gas, the reduced cyclotron motion is damped away and the situation is similar to the Figure 19. After the damping, ion motion is usually excited with the dipolar excitation at the magnetron frequency. Now the radius of the magnetron motion of all ions is increased and the quadrupole excitation can be started.

By applying the cyclotron frequency $\omega_c = \frac{q}{m_d}B$ of the desired ion as the oscillation frequency of the RF quadrupole field, the motion of the ions with mass m_d is converted from magnetron into reduced cyclotron motion. Due

to the buffer gas, reduced cyclotron motion is quite fast damped away and ions with mass m_d are driven into the center of the trap. This process is illustrated in Figure 20. By opening the potential wall at the extraction side of the purification trap, only the desired ions can be transferred into precision trap through the diaphraghm. Other ions will collide to the endcap electrode.

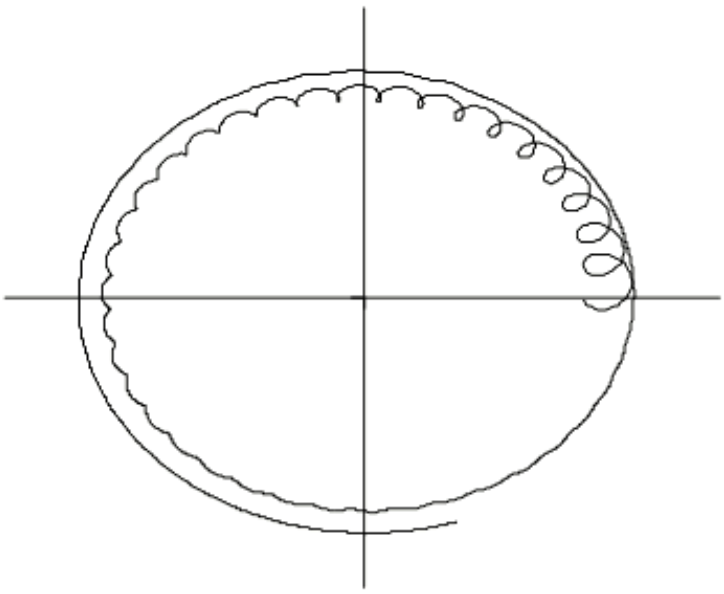

Figure 19: Damping of the eigenmotions of ions in a buffer gas filled Penning trap. [3]

6.3 Precision trap

Ions are injected into the precision trap in a similar way as in the case of the purification trap. Also the structure of the electrodes is similar to the purification trap, only the vacuum is better because the buffer gas is missing. In direct mass measurements the goal is to obtain the cyclotron frequency ω_c, and again the mass of ions as accurately as possible.

First, ions are located in the center of the precision trap and the radius of the magnetron motion is increased with dipole excitation with magnetron frequency ω_-. After that, quadrupole excitation is used, and if the excitation frequency $\omega_{ex} = \omega_c$, the magnetron motion will be completely converted to reduced cyclotron motion as it is shown in Figure 18. The frequency of the reduced cyclotron motion is much higher compared to the magnetron motion

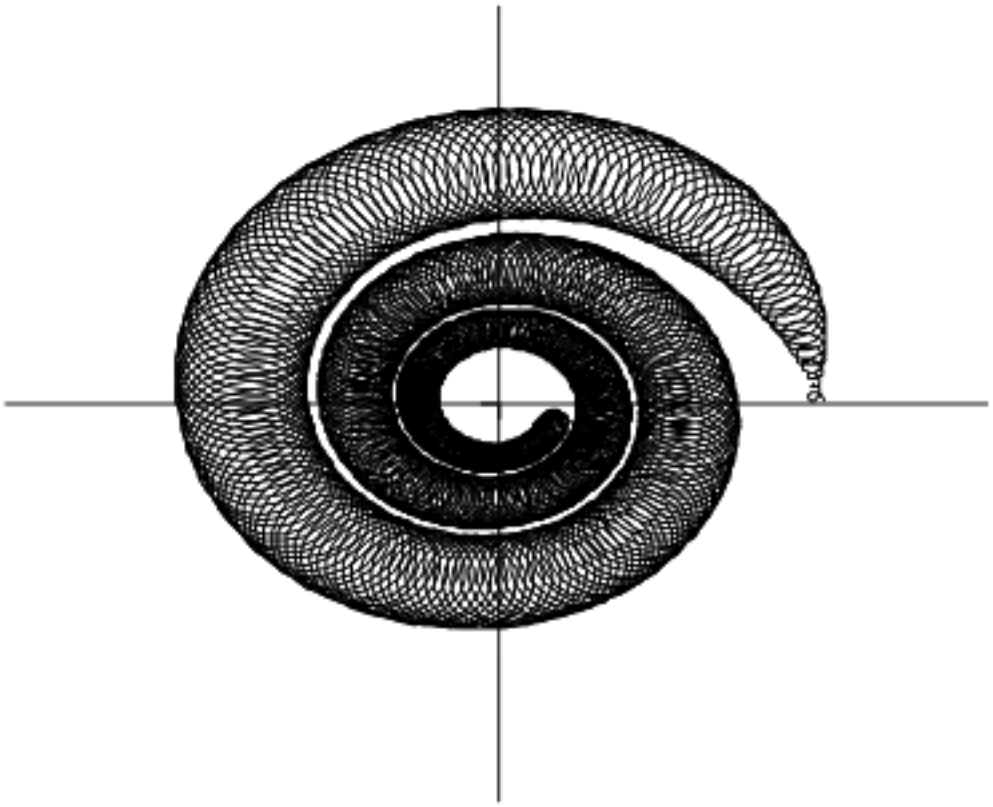

Figure 20: Conversion of the magnetron motion into reduced cyclotron motion with quadrupole excitation in a buffer gas filled Penning trap.

and therefore the radial energy of the ions is increased in this conversion. If the excitation frequency is not equivalent to the reduced cyclotron frequency the conversion will not be complete and the increase in radial energy will be smaller.

With a time-of-flight (TOF) technique [13] it is possible to detect changes in radial energy of the ions [16]. A micro-channel plate (MCP) detector is located in the beam line after the magnet and the time between releasing and detecting ions can be measured.

When the ion motion is converted to the reduced cyclotron motion, ions form small current loops which have magnetic moment $\vec{\mu}$. After opening the extraction side potential wall the magnetic moment of an ion interacts with the magnetic field gradient and an ion feels force [3]

$$\vec{F} = -\vec{\mu}(\vec{\nabla} \cdot \vec{B}) = -\frac{E_\rho}{B_t}\frac{\partial B(z)}{\partial z}\hat{e_z},$$

where E_ρ is the radial energy of the ion, B_t is the magnetic field in the region of the precision trap, $B(z)$ is the magnetic field at a given z-coordinate and $\hat{e_z}$ is a unit vector in z-direction. The force points in z-direction so the radial energy of the ion is converted into axial energy. The more the ion gets radial energy in the quadrupole excitation, the more it will gain axial energy in the extraction process.

By scanning the time-of-flights with different excitation frequencies, the time-of-flight minimum can be found. That corresponds to maximal radial energy and resonance excitation frequency. Time-of-flight with certain excitation frequency ω_{ex} can be obtained with the formula [3]

$$T(\omega_{ex}) = \int_{z_1}^{z_2} dz \left[\frac{m}{2(E_0 - qU(z) - E_\rho(\omega_{ex})B(z)/B}\right]^{\frac{1}{2}},$$

where m is the mass, E_0 the initial axial energy and q the charge of the ion. $U(z)$ is the potential and $B(z)$ the magnetic field at given z-coordinate. E_ρ is the radial energy of the ion with excitation frequency ω_{ex} and B is the magnetic field in the excitation region of the precision trap.

An example of a time-of-flight spectrum is illustrated in Figure 21. The accuracy of the measured time-of-flight depends on the FWHM (Full Width at Half Maximum) of the main peak. With longer excitation time it is possible to reduce the width of the resonance peak. However, in many cases, short halflives of the ions set a limit for increasing the excitation time.

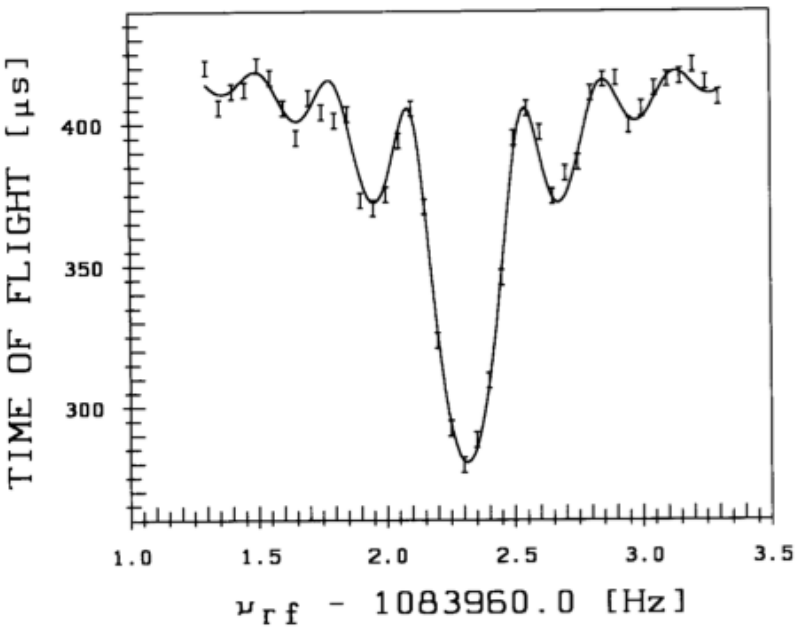

Figure 21: Example of a time-of-flight spectrum of ^{85}Rb ions. The excitation time is $T_{ex} = 3,6$ s and line width of the curve is $\Delta f(FWHM) = 0,28$ Hz. With this excitation time a resolving power $R = \frac{f}{\Delta f}$ of about four million is achieved. [13]

6.4 Ramsey method

Ramsey method means exciting ion motions with time-separated oscillatory fields. The method was invented by N.F. Ramsey in 1949 and is nowadays used in on-line Penning trap facilities. First time-separated ion excitations with Penning traps were done at ISOLTRAP in 1992 but today Ramsey method is also applied at JYFLTRAP. [17]

In the Ramsey method the excitation is divided into two or more parts so that the exciting pulses are phase coherent with each other. Usually the excitation is split into two parts and that is called two-fringe excitation. The exciting wave is switched on for time $\frac{1}{2}T_{RF}$, then switched off for time T_{WAIT}, and then again on for $\frac{1}{2}T_{RF}$. The amplitude of the exciting wave must be scaled with a factor $\frac{T_{RF}+T_{WAIT}}{T_{RF}}$.

With the Ramsey method a better mass resolution can be achieved compared to the conventional excitation method. As it is shown in Figure 22, the sideband structure is enhanced and the width of the main peak reduced with the Ramsey method.

Usually, mass of an ion is first measured roughly with normal excitation method without any time-separation in the exciting pulse. After that, the resonance spectrum pruduced by exciting ions with time-separated oscillatory fields. Now there is many peaks in the spectrum, but with help of the first rough mass measurement the main peak can be obtained.

6.4.1 Isomeric purification with time-separated oscillatory fields

The frequency resolution of the purification trap is approximately 10 Hz due to the buffer gas. Sometimes the ion bunch contains ion species having cyclotron frequency differences less than 10 Hz and they can not be separated in the purification trap. In this situation the whole bunch is transferred into the precision trap for better frequency resolution.

In the precision trap the Ramsey method can be used for even more accurate cleaning. The reduced cyclotron frequency of the unwanted isomer is excited with time-separated oscillatory field and it is removed from the trap center.

After the excition the potential wall between the traps is opened and the excited ions will collide to the electrode between the traps. The ions of interest

will pass through the diaphraghm into the purification trap.

In the purification trap the ions are cooled and re-centered due to another quadrupole excitation at cyclotron frequency. The essential property of the JYFLTRAP for this high-resolution cleaning to work is that the two penning traps are located inside the same magnet and therefore it is relatively easy to move ions back and forth between the traps.

For example, ions ^{115}Sn and ^{115}In having same mass to charge ratio have cyclotron frequency difference of about 4,5 Hz. [18] When an excitation time pattern of (10-80-10) ms (On-Off-On) is applied to these ions, the different isobars are fully separated.

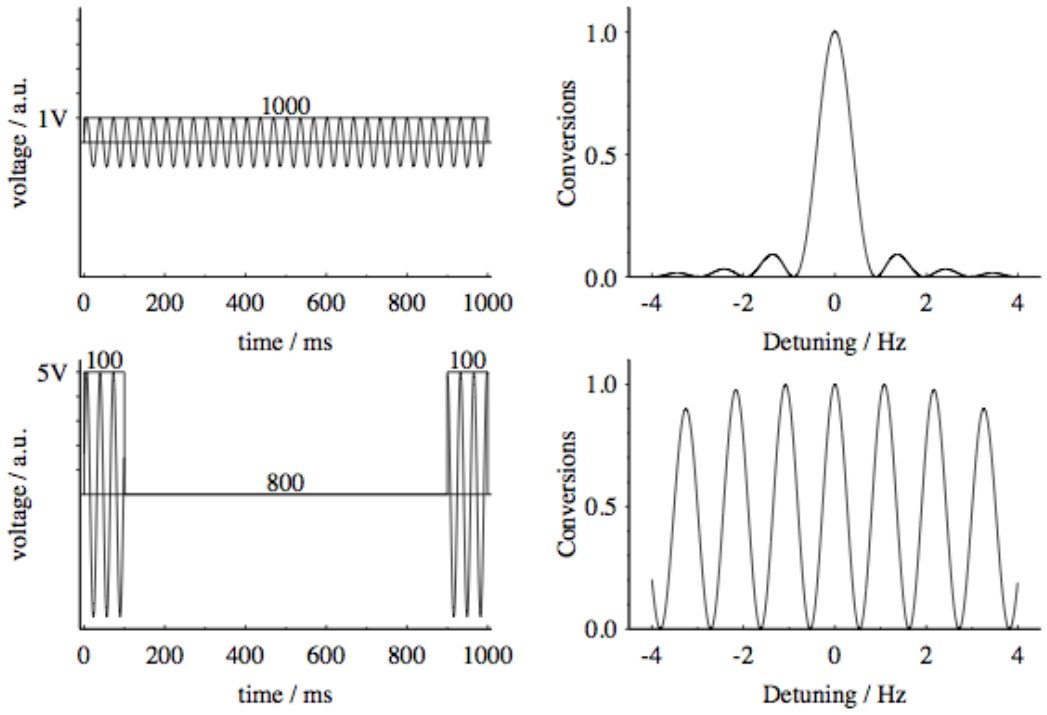

Figure 22: Time-separated and conventional excitation methods are compared. The longer is the time T_{wait} between excitation pulses, the larger has to be the excitation amplitude in the Ramsey method. The sideband structure is enhanced and the width of the main peak is reduced when ions are excited with time-separated oscillatory fields.

7 Electron motion along a magnetic field line

When an electron moves in a region where both electric and magnetic fields are present it feels the Lorentz force [8]

$$\vec{F} = -e(\vec{E} + \vec{v} \times \vec{B}) \tag{9}$$

where e is the electron charge, $\vec{E}$ the electric field, $\vec{v}$ the velocity of the electron and $\vec{B}$ the magnetic field. Magnetic force is written as $\vec{F} = -e(\vec{v} \times \vec{B})$ and it acts only on the velocity component perpendicular to the magnetic field. Due to the cross product the magnetic force only changes the direction of the velocity vector. This leads an electron into a circular orbit in a magnetic field. Radius of this circular orbit is written as

$$R = \frac{mv}{|e|B} \tag{10}$$

where m is electrons mass. This equation is derived by combining Newton's second law and the equation for the magnetic force.

In the experimental setup of the alignment the directions of electric and magnetic fields were installed as it is shown in Figure 23. In this situation electrons have both perpendicular and parallel velocity components to the magnetic field lines. This causes an electron to end up in a helical path and it will follow the same field line the whole way inside the vacuum tube. The radius of the helix can be obtained according to the equation (10) where v is the velocity component perpendicular to the magnetic field.

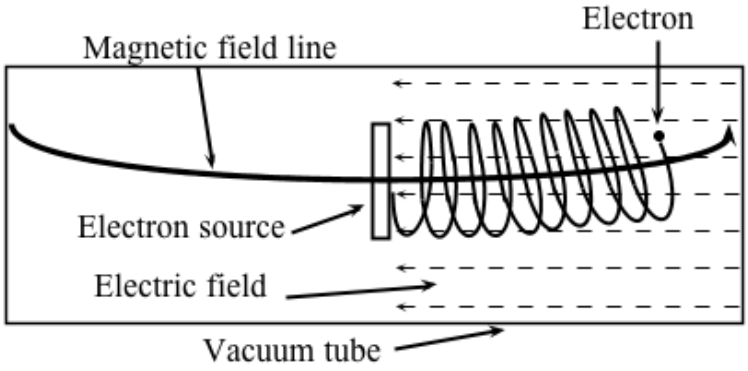

Figure 23: Electron motion along a magnetic field line.

8 Alignment equipments

Before the installation of the Penning traps it was necessary to align a vacuum tube inside the boretube of the superconducting solenoid [2]. This 7.0-T superconducting magnet with a warm bore with a diameter $D = 160$ mm and a length $L = 1012$ mm [3] is made by Magnex Scientific Ltd. Before the vacuum tube could be aligned the magnet had to be energized and shimmed and this was done by an engineer from Agilent Technologies Inc. In this case aligning means adjusting a vacuum tube inside the magnet until it is coaxial with the magnetic field lines. This was performed with a special alignment device.

8.1 Alignment device

A vacuum tube was inserted inside the magnet bore with adjustable supports at both injection and extraction side. With these adjustment pieces it was possible to turn the vacuum tube so that it would be coaxial to the magnetic field.

The alignment device consists of four rods and four plates with small holes in the middle. In the middle of the device there was a electron source as it is shown in Figure 24. A tungsten filament with a diameter $D = 0.8\,mm$ was used as the electron source. When there was a current through the filament it got warm and started to emit electrons. In order to accelerate electrons one applied a potential difference between the filament and the ground forcing electrons to travel along the magnetic field lines as it is described in section 7. At both injection and extraction side there was a segmented plate and there was a cable connected to every segment. Structure of one plate is illustrated in Figure 25. By measuring currents from every segment it was possible to find out which part of the plates electrons hit. And with the help of this information it was possible to determine in which direction the device should be moved. The main goal was to maximize the currents in both back plates.

First the distance between the segmented plates and the center plates was set to be $293\,mm$. Idea was to do the alignment in four phases and to move the plates farther from the center in every phase. That was done because the closer the plates are to the electron source the easier it is to find the right position for the tube. That is easy to understand with the help of Figure 26. Magnetic field lines will naturally diverge more when they are farther away from the magnet center. And because electrons will follow the field lines the electron spot that is observed is smaller and easier to detect when the plates

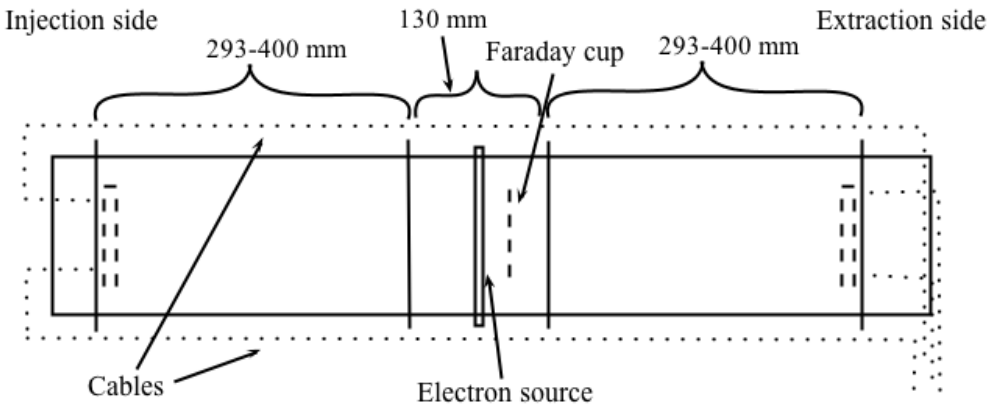

Figure 24: The structure of the alignment device is illustrated.

are closer to the center.

8.2 Setup for the alignment

After the device was inserted inside the magnet two plug chambers were fixed at the extraction side. The first plug chamber contained two 12 kV highvoltage feedthroughs which were used for feeding the current and the accelerating voltage into the vacuum as it is shown in Figure 27. After the second plug chamber containing three 10-pin feedthroughs for electrical connections for the collector plates was fixed the pressure inside the vacuum tube had to be pumped low enough. Edwards turbomolecular pump *STP-301* and Edwards *XDS 35i* prepump were used for pumping. Two different pressure sensors were used for pressure monitoring. Those were Varian Sensor (Pressure) *FRG-720* and Varian Lexington *MA02421 AGC-100*.

The large current through the electron source was created with POWER delta elektronika power supply. A Kikusui power supply was used for accelerating voltage which was 100 V. In order to create an accelerating electric field for the electrons the electron source was connected to lower and ground to higher potential as it is shown in Figure 28. Currents from the segmented plates were measured with both analog and digital picoammeters. Used devices were Keithley digital *IEE488* and analog *414A* picoammeter.

A plug chamber was fixed at the extraction side and it is illustrated in Figure 29. Inside the plug chamber there were sockets which were connected to the

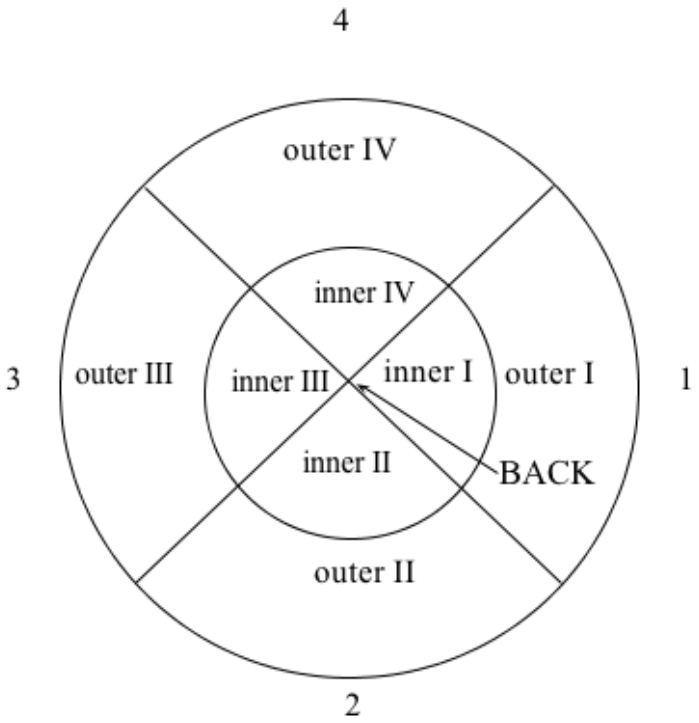

Figure 25: Structure and numbering of segments of the plate at the injection side.

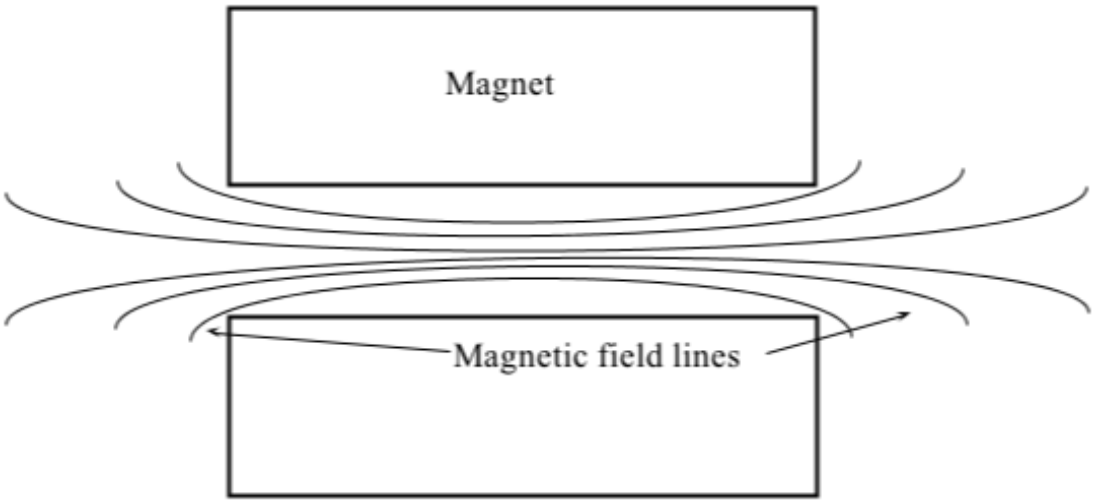

Figure 26: Divergence of the magnetic field lines inside the magnet.

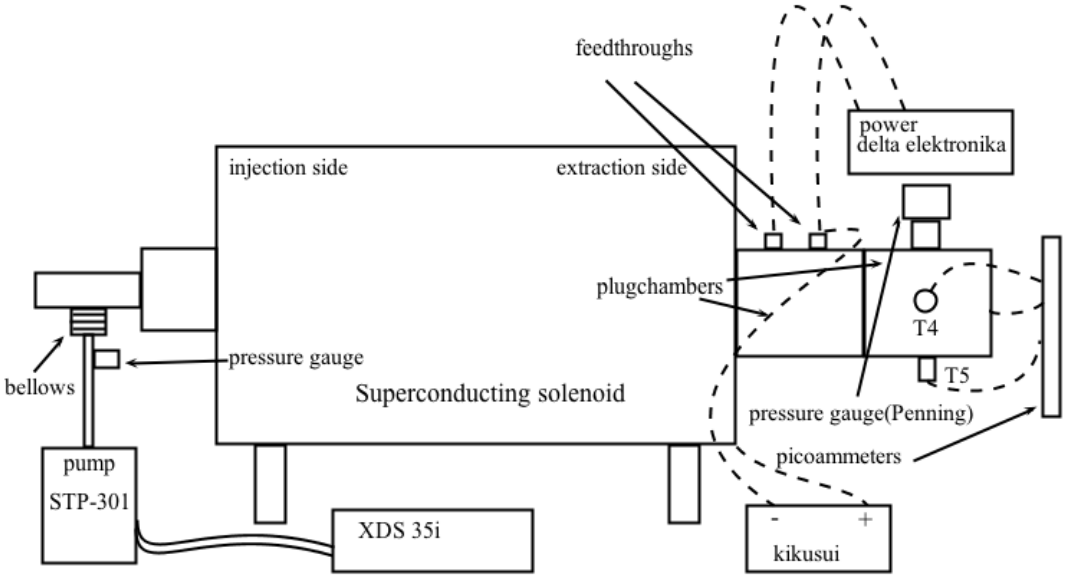

Figure 27: A schematic drawing of the alignment setup.

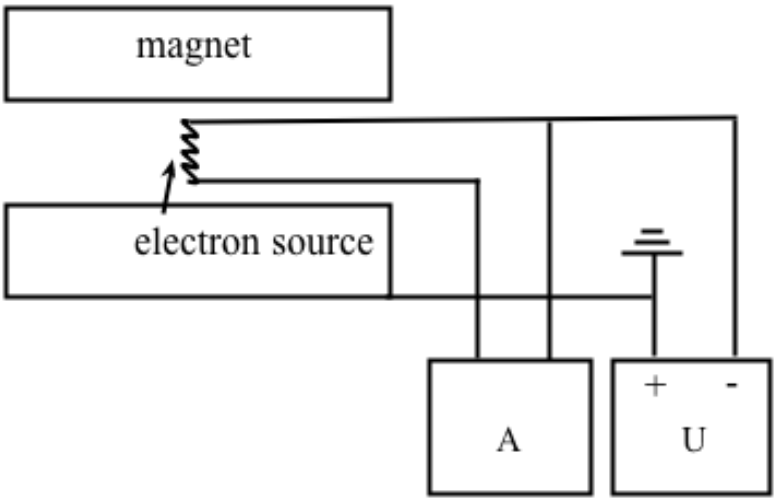

Figure 28: The connections of the power supplies.

plugs. The structure of those is shown in Figure 30. The wires from the segmented plates of the alignment device were connected to the plugs with pins which went into the sockets of the plug chamber. The connections are shown in Table 1.

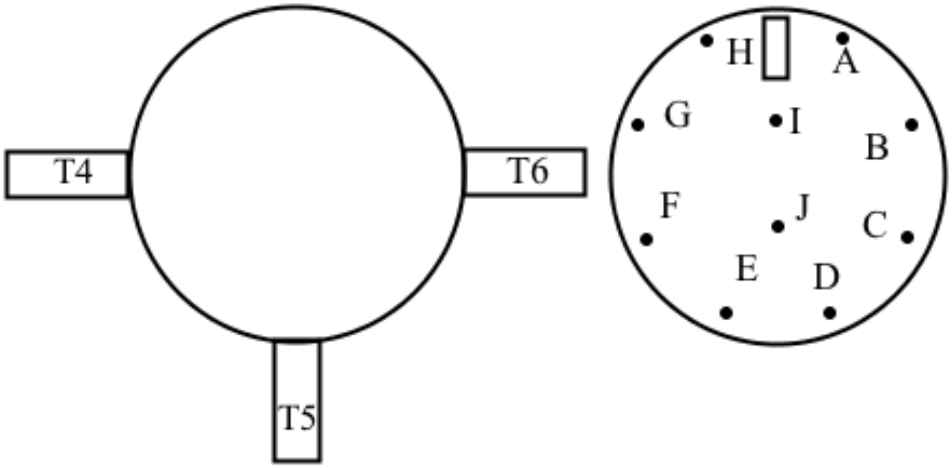

Figure 29: Plug chamber at the extraction side. Also structure of one plug is illustrated.

Table 1: The connections between the segmented plates and the sockets in the plug chamber.

Extraction side	Injection side
outer 1 (T5B)	outer 4 (T6A)
outer 2 (T5A)	outer 1 (T5F)
outer 3 (T5D)	outer 2 (T6C)
outer 4 (T4H)	outer 3 (T5E)
inner 1 (T5H)	inner 4 (T6F)
inner 2 (T4F)	inner 1 (T5G)
inner 3 (T4G)	inner 2 (T6H)
inner 4 (T4I)	inner 3 (T6B)
BACK (T5C)	BACK (T6E)
	FC (T6G)

9 Electron mean free path

In order to find out how good vacuum was needed to pump it was necessery to calculate an estimation for the mean free path of an electron. In higher

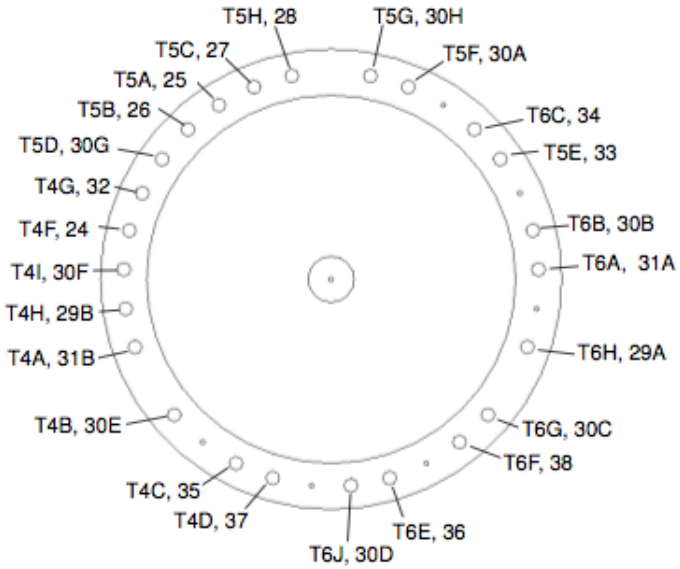

Figure 30: The sockets inside the plug chamber.

pressure an average path travelled by electron is shorter than in lower pressure. The length of the vacuum tube was approximately $1\,m$ so the order of magnitude of the mean free path had to be at least some metres. The mean free path is given by [19]

$$\lambda = \frac{1}{n_V \sigma} \tag{11}$$

where n_V is the number of particles of the medium in a volume unit and σ is the cross section. In this estimation geometric cross section

$$\sigma = \pi r^2 \tag{12}$$

has been used. This is an area determined by the interaction radius which in this estimation is nitrogen atom (^{14}N) radius $r = 70\,pm$. Nitrogen radius has been used because electron radius is small in comparison to the molecules of the air and those are mostly nitrogen. Pressure was also needed to place in equation (11) and that was done with the help of ideal gas law

$$PV = nRT \tag{13}$$

where P is the pressure, V the volume, n the amount of substance of the gas in moles, R the gas constant and T the temperature. Since Avogadro constant N_A is the amount of particles in one mole n can be written $n = \frac{N}{N_A}$ where N is

the number of particles. Now after replacing n with N and N_A equation (13) gives

$$\frac{N}{V} = \frac{N_A P}{RT}. \tag{14}$$

Since $n_V = \frac{N}{V}$ the combination of equations (11), (12) and (14) gives

$$\lambda = \frac{RT}{N_A P \pi r^2}. \tag{15}$$

By using room temperature and pressure $P = 10^{-4}\,mbar$ equation (12) gives $\lambda \approx 0,26\,m$ and with pressure $P = 10^{-5}\,mbar$ $\lambda \approx 2,6\,m$ for the mean free path of an electron. So according to these calculations pressure had to be pumped at least as low as $10^{-5}\,mbar$. The temperature of course rises when the filament is heated but this gives a rough estimation.

10 Experimental methods

When the vacuum tube was inside the magnet and the pressure had been pumped low enough it was possible to start to increase the current through the electron source filament. The increasing of the current was done slowly, 2 amperes in every 5 minutes. When the current reached $25\,A$ an electron current in the Faraday cup (FC) was observed. However the current was increased up to $27,4\,A$ to get more beam. It was also necessary to be careful because the filament might have easily burned with too high current.

The accelerating voltage was connected in such a way that the filament was in negative potential and the rest of the tube in positive potential. Hence the electrons would be accelerated in the electric field towards the ends of the tube.

Initial position of the tube was adjusted by a ruler. Then currents from all the segments of the alignment device were measured. In the beginning there were not much current but after a little adjustment large currents were observed. The problem was that in the injection side the beam hit a little bit up from center and in the extraction side it hit straight to the back plate. Many hours were spent trying to fix this imperfection but no improvements were observed.

10.1 Scanning method

Since the previous technique gave no results a more organized scanning method was tested. The tube was first lowered in the lowest possible position and the currents were measured. Then every adjustment piece was turned one turn up and the currents were measured again. This was repeated until the tube was clearly gone past the magnet center. From the results it was easy to conclude that the tube was placed little bit too much to the left when looking from the extraction side. Because of that the tube was lowered down again but now it was moved little bit to the right before a new scan was started.

Four scans with different starting points were done and then it was necessary to search the best position of the tube for later adjustment. After all, it was decided that the best situation for finetuning was found from the first scan when each adjustment piece had been turned 9 turns up. The tube was adjusted to this position and after a little finetuning there was $42\,nA$ in the injection side back plate and $38\,nA$ in the extraction side back plate and almost zero amperes in the other segments.

10.2 Second and third phase

After the scanning the device was taken out and the back plates were moved farther away from the center. The right position of the tube was searched again with the adjustment pieces. This was done two times and final distance between the back plates and the center of the device was 400 mm.

10.3 The fourth phase

For the final phase of the alignment process the device was taken out and the segmented plates were removed. This was done to minimize all the disturbance those plates might cause to the measured currents in the back plates. Device was inserted back in and the right position was found quite fast. Measured currents were $10\,nA$ at both injection and extraction side. The final positions of the adjustment pieces is illustrated in Figures 31 and 32.

11 Improvements for the trap system

Few improvements were done for the electrodes which form the Penning traps in JYFLTRAP. The electrodes with the diaphragms at both ends of the

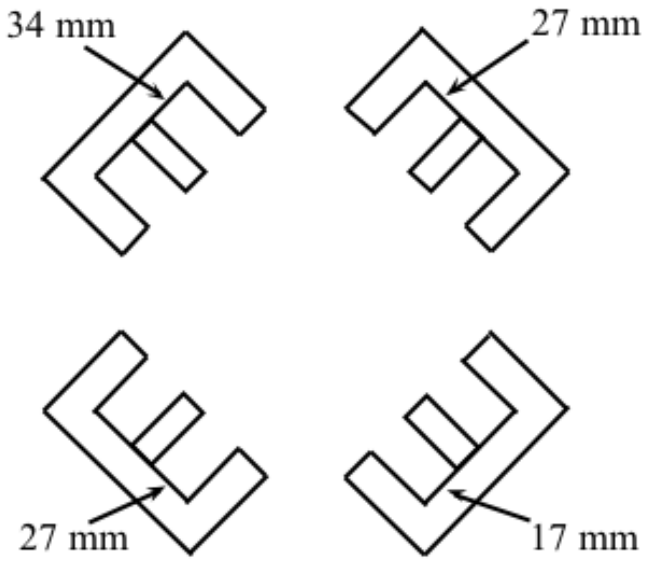

Figure 31: Position of the adjustment pieces at the extraction side after the alignment process was completed.

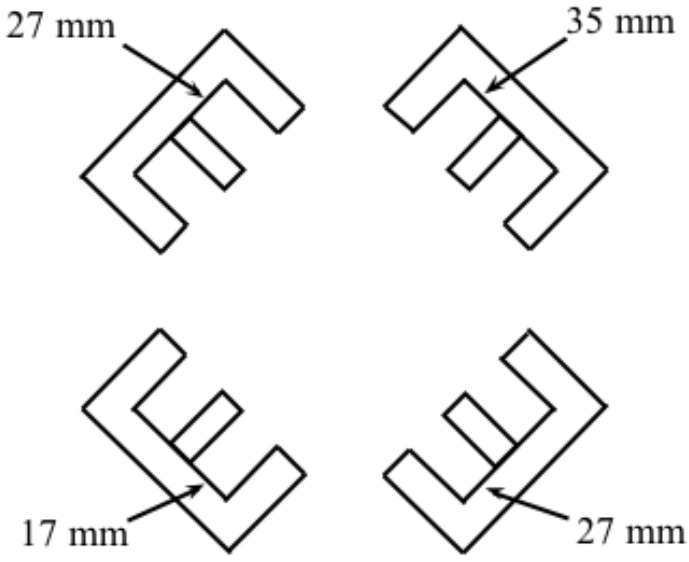

Figure 32: Position of the adjustment pieces at the injection side after the alignment process was completed.

purification trap were changed. The idea was to get smaller diaphragms so that the buffer gas flow from the purification trap would be minimized. The size of the injection side diaphragm was decreased from 4 mm to 3 mm and the diameter of the electrode between the traps was decreased from 2 mm to 1,5 mm.

A new pumping barrier was installed to prevent the buffer gas flow to the presicion trap. A drawing of the new pumping barrier is shown in Figure 33. Also a new gas line for buffer gas feeding was built. The diameter of the new gas tube is wider compared to the previous one which permits more efficient gas flow to the purification trap. One electrode of the purification trap had to be changed because of the attachment of the new gas line. A drawing of the improved Penning traps is shown in Figure 34 and a photograph is shown in Figure 35. The structure of the gasline outside the magnet is illustrated in Figure 36. The gasline was built with Swagelok and VCR connectors.

Figure 33: New pumping barrier. After the trap was pushed inside the magnet the three bolts in the pumping barrier were tightened. The teflon o-ring around the pumping barrier was pushed outwards and it should prevent the gas flow effectively.

When the magnet was shimmed the regions of the homogeneity were of a little bit different place compared to the previous settings at IGISOL-3. The new locations of the regions of homogeneity are 414,6 mm and 614,6 mm (measured from the injection side of the magnet). That means, that the location of the traps inside the magnet had to be changed and new spacers had to be made at the both ends of the trap system. The injection side spacers are illustrated in Figure 37. The spacers define the location of the traps as they are pushed inside the magnet.

11.1 Installation of the Penning traps

After the alignment and the improvements, the Penning traps were ready for the installation inside the magnet. The new bumping barrier had to be tightened after the traps were pushed inside because otherwise the pushing would have been impossible. This was done with special long allen key. The building of the new gasline was finished after the traps were installed.

12 Electrical connections of the trap electrodes

Electrical connections of the injection side electrodes were changed from the previous trap system. New connections are shown in Figure 38. Electrical connections of the extraction side trap electrodes are shown in Figure 39.

Also the three extraction electrodes which are illustrated in Figure 40 were connected to extraction plug chamber. The connections between them and the sockets in the plug chamber are listed in Table 2.

Table 2: The connections between the extraction electrodes and the sockets in the plug chamber.

Extraction electrode	Connection in plug chamber
1	T4J
2	T5J
3	T6D

13 Simulations

A commercial SIMION program [20] was used to simulate ion trajectories from the RFQ cooler to the Penning traps. With SIMION it is possible to build

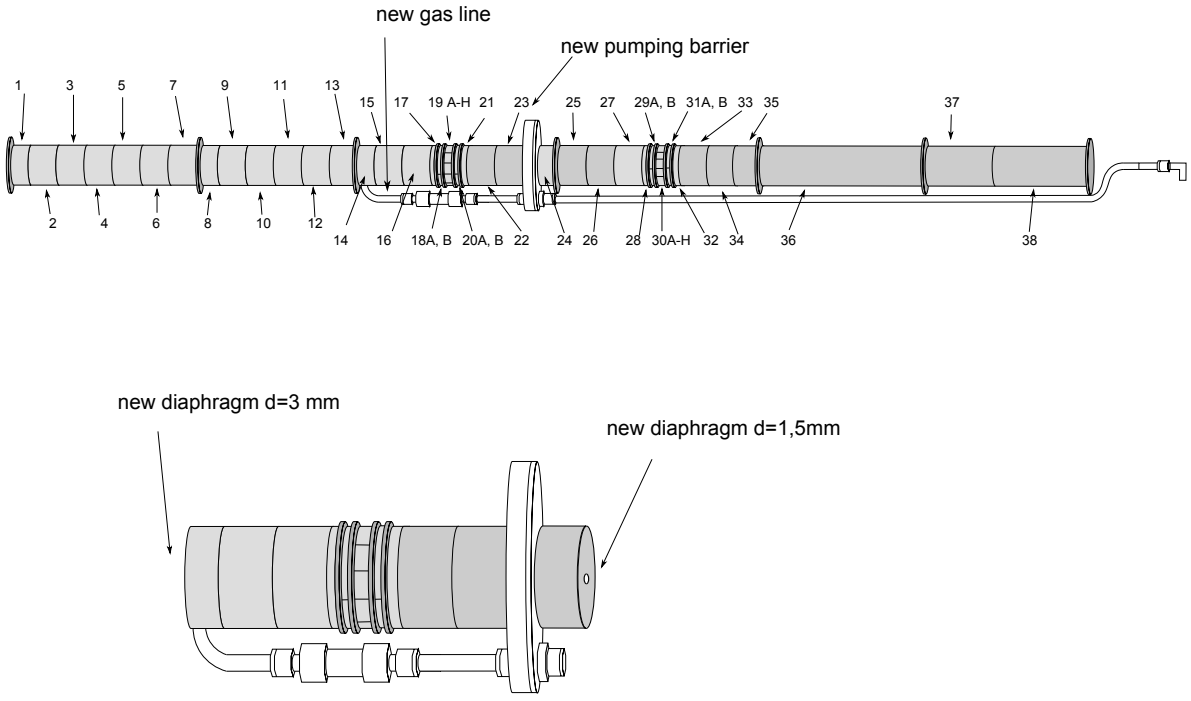

Figure 34: The structure of the improved Penning traps.

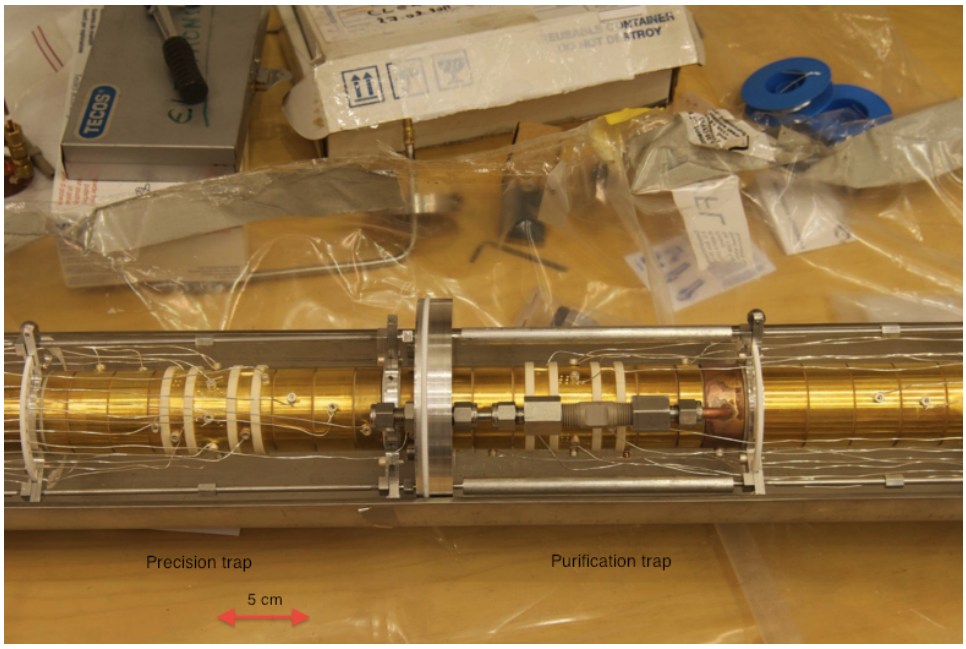

Figure 35: A photograph of the improved Penning traps.

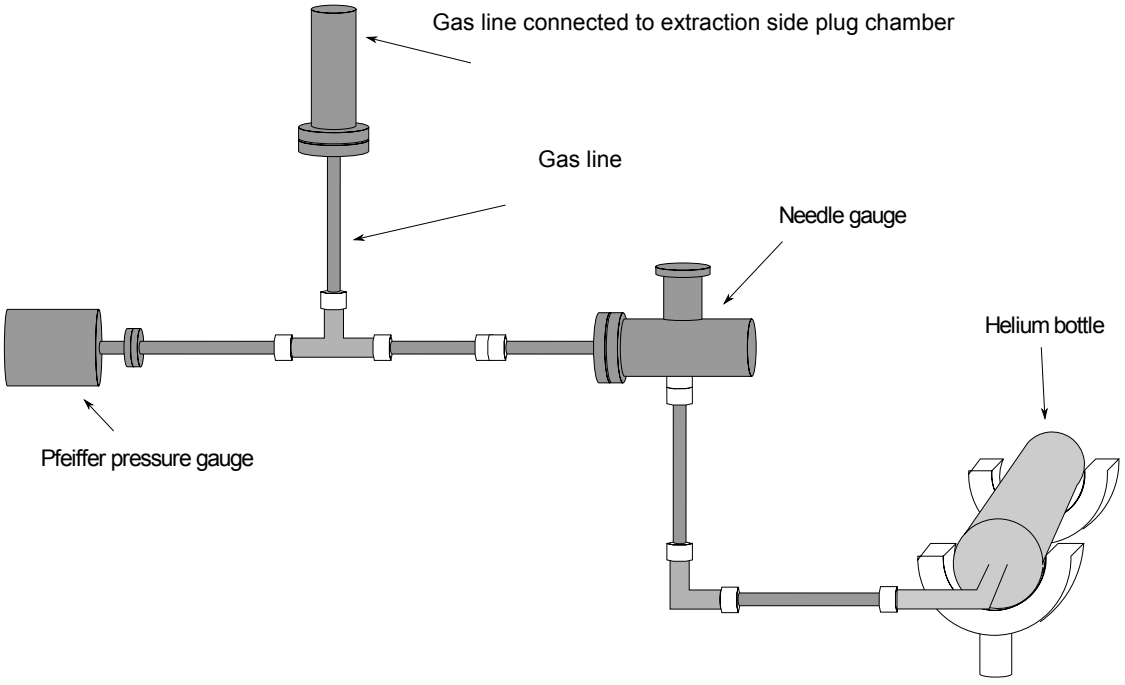

Figure 36: Gas line outside the magnet.

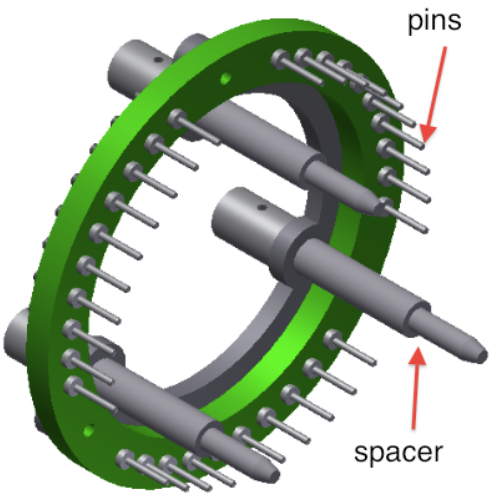

Figure 37: Spacers and pins at the injection side of the trap. The structure of the pins and spacers at the extraction side is the same. Spacers at the injection side define the location of the traps inside the magnet.

a simulation of the beam line with necessary ion optics and ion source. Then the voltages of the ion optics can be adjusted so that all the ions are transported through the simulated beam line. With these simulated voltages it is easier to start to tune the beam for the real experiments.

Simulated beam line from cooler to trap is shown in Figure 41. The ion optics after the Penning traps are illustrated in Figure 42. Some of the voltages for the ion optics were estimated using simulations and some were estimated using values from the previous experimental setup.

Simulated voltages for the ion optical elements are listed in Table 3 in Appendix A. Voltages from the previous experimental setup are listed in Table 4. Voltage of the Einzel lens is applied to the center electrode while two other electrodes are in ground potential.

In Tables 3 and 4 there are also listed proposed power supplies for the electrodes. Proposals are done corresponding to supplies which are left from the old laboratory. With these power supplies there is no need for new ones but there are couple questionable power supplies in that list. The -500 V -Isegs

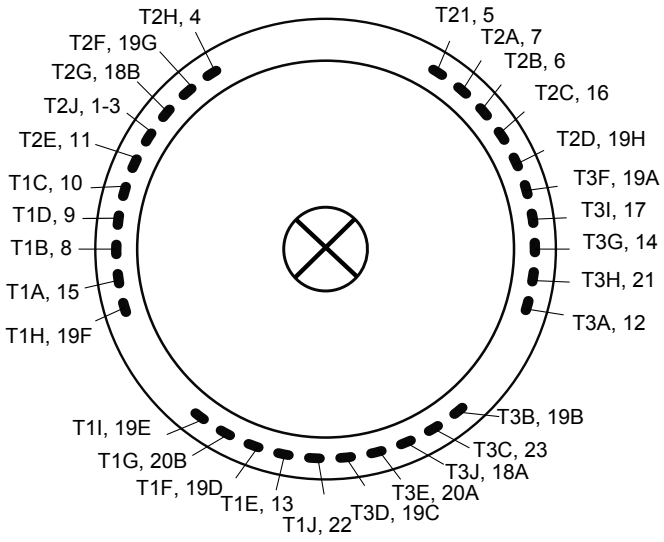

Figure 38: Electrical connections of the injection side trap electrodes.

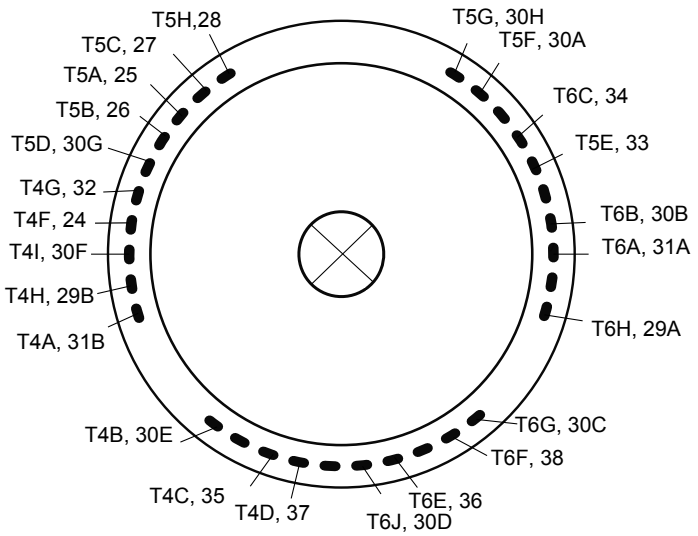

Figure 39: Electrical connections of the extraction side trap electrodes.

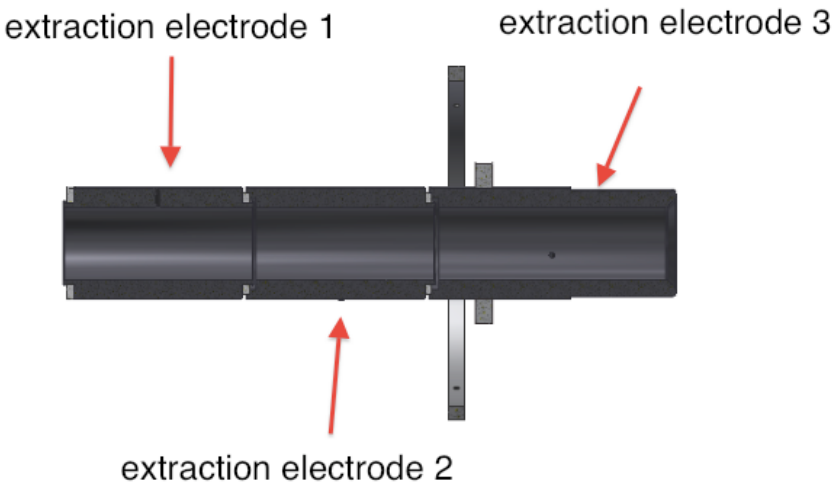

Figure 40: Extraction electrodes.

are not the best choices for Einzel 3 and Einzel 5 so it is maybe necessary to order some new power supplies.

The ion optics are created in SIMION by using geometry files (gem-files). A gem-file is created with a text-editor and gem-files which were used to create an Einzel-lens and 90 degree bender are shown in Appendix B. In the gem-file of the Einzel lens the lenghts of the electrodes are 150 units, 30 units and 48 units. By varying this file it is easy to create different Einzel lenses.

14 Conclusions

During years 2011 and 2012 the IGISOL facility has been moved to a new location and the building of the laboratory has been started from zero point. The subject of this thesis was the initialization of the Penning traps and it was done during these years. In the summer of 2011 the magnet was installed, turned on and aligned. And in the summer of 2012 the Penning traps were improved and installed.

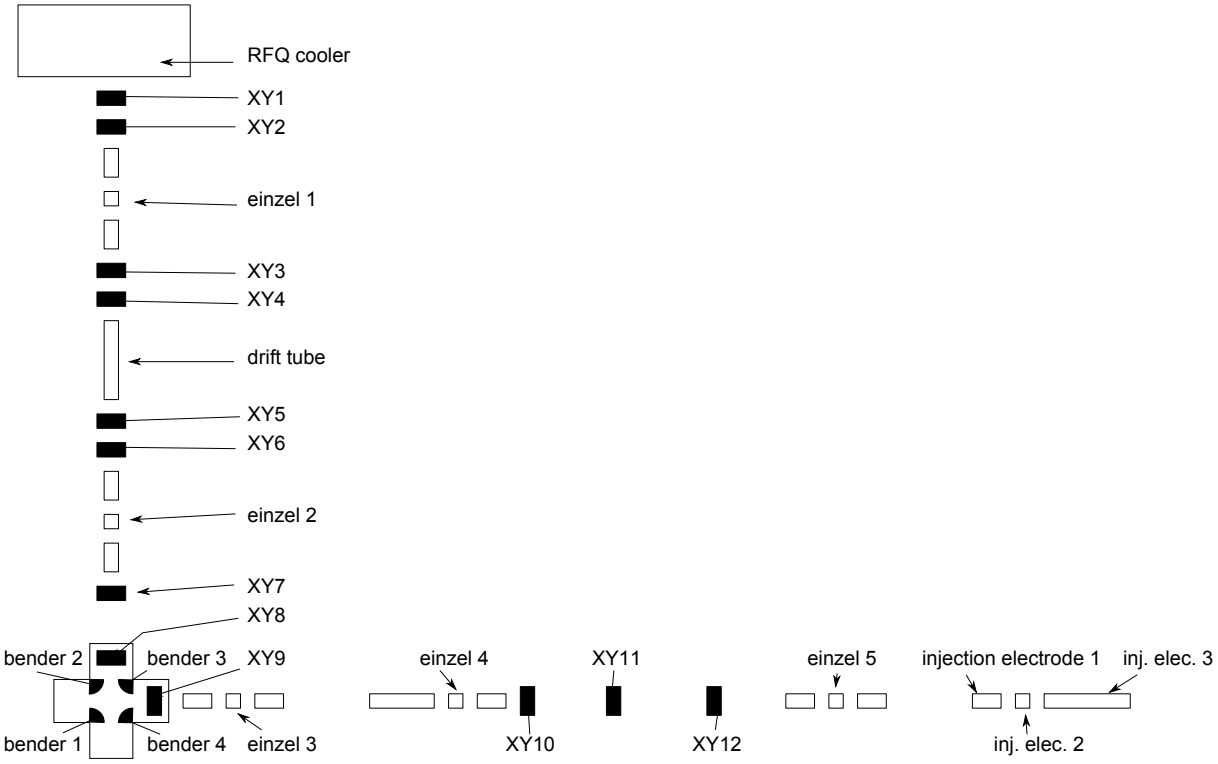

Figure 41: Ion optics in the new beam line between the RFQ cooler and the Penning traps.

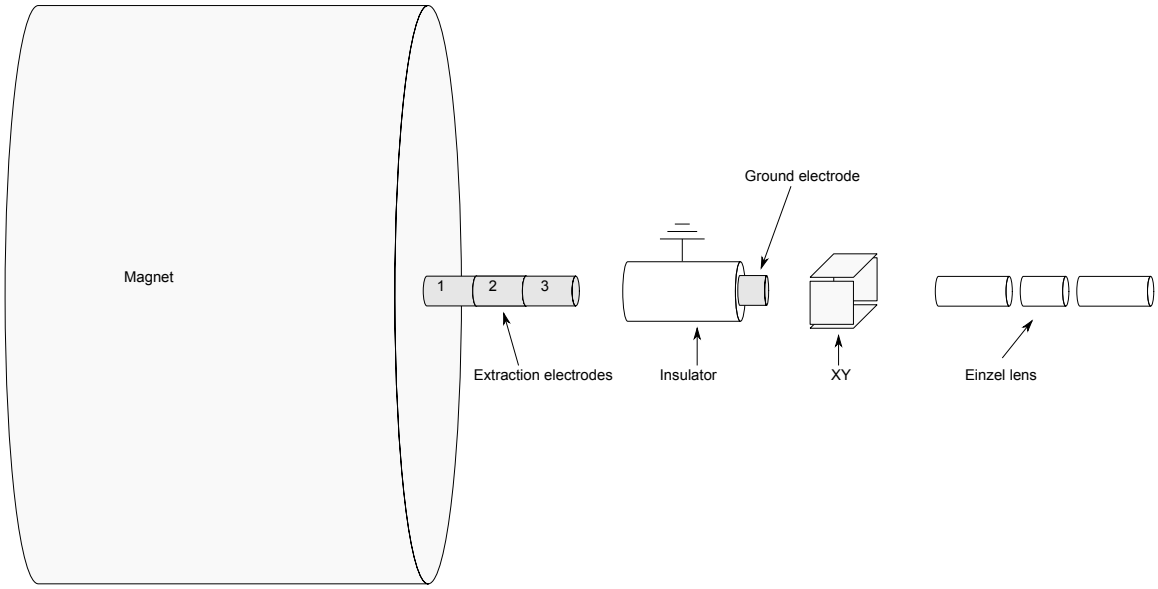

Figure 42: Ion optics in the beam line after the Penning traps.

14.1 Alignment

It was observed that when the distance between the segmented plates and the center plates was set over $400\,mm$ the current was fluctuating between all the segments. The fluctuating caused difficulties to the measurements and therefore $400\,mm$ was decided to be the final distance between the plates. This distance was long enough also considering the length of the warm bore inside the magnet which is $L = 1012\,mm$.

It is possible to estimate the maximal fractional shift of the cyclotron frequency caused by the misalignment between the magnetic field axis and the trap axis. This fractional shift for small imperfections with $\theta \ll 1$ and $\epsilon \ll 1$ is determined by [21]

$$\frac{\delta\omega_c}{\omega_c} = \frac{9\alpha^4\theta^2}{16} - \frac{\alpha^4\varepsilon^2}{8}, \tag{16}$$

where $\alpha = \frac{\omega_z}{\omega_+}$, ω_z is the axial frequency, ω_+ is the reduced cyclotron frequency, θ is the maximum misalignment angle between the magnetic field axis and the trap axis and ε is the asymmetry parameter of the electric field. For ions with charge $q = 1e$ and mass number $A = 100$ the cyclotron frequency in a $7\,T$ magnetic field is $\omega_c = 6753972\,Hz$ according to equation

(6). Since the magnetron frequency at JYFLTRAP is approximately 1700 Hz [10] equation (8) gives for the reduced cyclotron frequency $\omega_+ = \omega_c - \omega_- = 6752271\,Hz$. Now equation (7) gives $\omega_z = 2\sqrt{\frac{\omega_c^2}{4} - (\omega_+ - \frac{\omega_c}{2})^2} = 214279\,Hz$. While estimating the maximum misalignment angle it is assumed that the center of the alignment device is located on the field axis. The distance between the center of the aligment device and the segmented plates was 400 mm in the final phase of the alignment. Since the diameter of the pinhole in the middle of the detector plate is $D = 0,2\,mm$ both ends are certainly misaligned less than 1 mm and the maximum misalignment angle is $\theta = arcsin\frac{1}{400} = 0,0025\,(rad)$. When assuming the electrode asymmetry as large as $\varepsilon = 0,01$ ($|\varepsilon| = 1$ %) [21] and using these calculated values for the frequencies and the angle equation (16) gives $3,6 \cdot 10^{-12}$ for first term and $1,3 \cdot 10^{-11}$ for the second term of the fractional shift of the cyclotron frequency. The expected accuracy of the Penning trap system is of the order of 10^{-8} so the remaining misalignment will not have any significant effects to the future experiments.

14.2 Penning traps

The Penning traps are the same which were used in the previous IGISOL facility. Only few improvements were done for the traps. The pumping barrier was replaced with a tighter one. Also electrodes with diaphraghms were changed to electrodes with smaller diaphraghms to diminish the gas flow out of the purification trap. New gas line with a wider tube was built to make the buffer gas feeding more effective. For these changes the trap electrodes had to be taken apart almost completely and that took quite a long time.

After changing the new spacers, it was noticed that the old cables were not long enough at injection side. So also new cabling had to be done for the whole trap system. This caused some troubles because the bolts were old and they broke very easily inside the electrodes.

Also the aluminium sticks which were holding the electrode packages together broke very easily and it was hard to handle them. For the next trap upgrade these sticks could replaced with more solid ones.

During these procedures some connections were observed between the trap electrodes. Especially the new gas feeding electrode at the purification trap which was not gold-plated was continuosly connected to the electrode next to it. There was maybe some particles coming out of it which caused the connections. However, there were not any connections observed as the traps were put inside the magnet.

Appendix A

Estimated voltages

The RFQ and the magnet are located on the 30 kV high voltage platform and the voltage of the line is lowered by 900 V. Due to the fact that the zero voltage level in Table 3 is 30 kV, the voltage of the beamline is -900 V. On this scale the power supplies are in zero potential (30 kV compared to real ground) and they lower the voltage from that level.
Also in Table 4 the zero voltage level is 30 kV but there is one exception. The zero voltage level of the extraction einzel is real ground. Therefore the middle electrode of the extraction einzel is connected to positive voltage.

Table 3: Simulated voltages for the ion optics in the beam line between the RFQ and the Penning traps.

Element	Simulated voltage	Proposed power supply
einzel 1	-500 V	-1 kV Spellman
einzel 2	-560 V	-1 kV Spellman
bender 1	0 V	1 kV Spellman
bender 2	-170 V	-2 kV Spellman
bender 3	-166 V	-2 kV Spellman
bender 4	-800 V	-5 kV Spellman
einzel 3	-470 V	-500 V Iseg
einzel 4	-590 V	-1 kV Spellman
einzel 5	-500 V	-500 V Iseg

Table 4: Voltages estimated using the values from the previous experimental setup. -1 kV Iseg power supply is proposed for all the xy-steerers.

Element	Estimated voltage	Proposed power supply
inj. elec. 1	-900 V	
inj. elec. 2	-400 V	-500 V Iseg
inj. elec. 3	-350 V	-500 V Iseg
extr. elec. 1	-100 V	-500 V Iseg
extr. elec. 2	-200 V	-500 V Iseg
extr. elec. 3	-1200 V	-3 kV Spellman
X_n		-1kV Iseg
Y_n		-1kV Iseg
extr. einzel	12 kV	20 kV Spellman

Appendix B
Geometry files

Geometry files for creating an Einzel lens and 90 degree bender are shown. With these gem-files SIMION-program can create these electrode structures. By applying these files it is possible the create the beam line from the RFQ to the magnet and simulate the voltages that are needed to guide and focus the ion beam.

```
; Einzel lens geometry file
PA_define (248,30,1,c,y,e)
; tekee 3D cylinteri ja y symmetriat
Locate(0,0,0,1,90,0,0);origo kuvalle
 {

 ;-----------------------------------------------------

Electrode(1)
 ;ion source extraction ja tube
  {
  Fill
        {
         within{cylinder(0,0,150,18,18,150)}
         notin{cylinder(0,0,150,15,15,150)}

        }
  }


 ;-----------------------------------------------------
Electrode(2)
 ;ion source extraction ja tube
  {
  Fill
        {
         within{cylinder(0,0,190,18,18,30)}
         notin{cylinder(0,0,190,15,15,30)}

        }
  }

;-----------------------------------------------------
Electrode(3)
 ;ion source extraction ja tube
  {
  Fill
        {
         within{cylinder(0,0,248,18,18,48)}
         notin{cylinder(0,0,248,15,15,48)}

        }
  }

}
```

```
; quadrupole beam bender geometry file
PA_define (200,200,100,planar, non-mirrored)
Locate(100,100,0,1,0,0,0);origo kuvalle
 {
;-------------------------------------------------------
Electrode(1)
; Bending rod 1
  {
  Fill
        {
         within{cylinder(-55,-55,100,35,35,100)}
         notin{corner_box3d(-100,-100,0,45,90,100)}
         notin{corner_box3d(-100,-100,0,90,45,100)}
         }
  }
;-------------------------------------------------------
Electrode(2)
; Bending rod 2
  {
  Fill
        {
         within{cylinder(-55,55,100,35,35,100)}
         notin{corner_box3d(-100,0,0,45,100,100)}
         notin{corner_box3d(-100,55,0,100,45,100)}
        }
  }
;-------------------------------------------------------
Electrode(3)
; Bending rod 3
  {
  Fill
        {
         within{cylinder(55,-55,100,35,35,100)}
         notin{corner_box3d(0,-100,0,100,45,100)}
         notin{corner_box3d(55,-100,0,100,100,100)}
        }
  }
;-------------------------------------------------------
Electrode(4)
; Bending rod 4
  {
  Fill
        {
         within{cylinder(55,55,100,35,35,100)}
         notin{corner_box3d(0,55,0,100,45,100)}
         notin{corner_box3d(55,0,0,100,100,100)}
        }
  }
;-------------------------------------------------------
}
```

References

[1] E. Kugler, Hyp. Int. **129** (2000) 23 .
[2] J. Äystö, Nucl. Phys. A **693** (2001) 477.
[3] V. Kolhinen, PhD Thesis (2003).
[4] W. F. G. Swann, Phys. Rev. **44** (1933).
[5] A. Adams and F. H. Read, J. Phys. E (1972).
[6] A. Jokinen et al., Int. J. Mass Spectrom. **251** (2006) 204.
[7] P. Karvonen et al., Nucl. Instrum. Methods Phys. Res. B **266** (2008) 4794.
[8] H.D. Young and R.A. Freedman, *University Physics with modern physics*, 11th edition, Addison Wesley Longman (2004).
[9] A. Nieminen et al., Phys. Rev. Lett. **88** (2002) 094801-1.
[10] V. Kolhinen, et al., Nucl. Instrum. Methods Phys. Res. A **528** (2004) 776.
[11] J.A. Hipple, H. Sommer and H.A. Thomas, Phys. Rev. **76** (1949) 1877.
[12] G. Bollen et al., Nucl. Instrum. Methods A **368** (1996) 675.
[13] M.König, G.Bollen, H.-J.Kluge, T. Otto, J.Szerypo, Int. J. Mass Spectrom. **142** (1995) 95.
[14] Tommi Eronen et al., Eur. Phys. J. A **48** (2012) 46.
[15] Tommi Eronen, MSc Thesis (2003).
[16] U. Hager, V.-V. Elomaa, T. Eronen, J. Hakala, A. Jokinen, A. Kankainen, S. Rahaman, S. Rinta-Antila, A. Saastamoinen, T. Sonoda, and J. Äystö, Phys. Rev. C **75** (2007) 064302.
[17] Tommi Eronen, PhD Thesis (2008).
[18] T. Eronen et al., Nucl. Instrum. Methods Phys. Res. B **266** (2008) 4527.
[19] J.S. Lilley, *Nuclear Physics, Principles and Applications*, John Wiley & Sons Ltd (2001).
[20] D. Manura, D. Dahl, *SIMION (R) 8.0 User Manual*, Scientific Instrument Services, Inc. Ringoes, NJ 08551 (2008).
[21] L.S. Brown and G. Gabrielse, Rev. Mod. Phys. **58** (1986) 233.